CARDIOVASCULAR TISSUE ENGINEERING:

BIOPHYSICAL STIMULATION AND MATURATION OF CARDIAC RINGS

RECELLULARIZED WITH HUMAN CARDIOMYOCYTES

A Dissertation

by

KARIS RACHEL TANG-QUAN

Submitted to the Office of Graduate and Professional Studies of
Texas A&M University
in partial fulfillment of the requirements for the degree of

DOCTOR OF PHILOSOPHY

Chair of Committee,	Ken Muneoka
Co-Chair of Committee,	Doris A. Taylor
Committee Members,	Robert C. Burghardt
	John C. Criscione
Head of Department,	Larry J. Suva

August 2019

Major Subject: Biomedical Sciences

ABSTRACT

Cardiovascular diseases that often result in end-stage heart failure continue to disable and take patient lives around the world. In an effort to provide new therapeutic options for patients waiting for a heart transplant, scientists, clinicians, and engineers are working toward engineering cardiovascular tissue. Three essential components in tissue engineering are the scaffolds, cells, and signals. In this dissertation, I focused on using the decellularized cardiac extracellular matrix as a bioscaffold for creating functional cardiac tissue. In Chapter 2, we increased cell retention during recellularization using the biomaterial gelatin in the whole decellularized rat heart. Following these recellularization studies of rat cardiomyocytes in rat hearts, we moved toward establishing a model for studying cardiomyocytes in cardiac extracellular matrix under mechanical and electrical stimulation. In Chapter 3, I created cardiac rings by recellularizing rat cardiac extracellular matrix or rat collagen to investigate the effects of the matrix material on cardiomyocyte contractility and cell elongation. In Chapter 4, I moved to a more clinically translatable model of using human induced pluripotent stem cell-derived cardiomyocytes in human pediatric-sized cardiac rings made from decellularized rabbit hearts. These human pediatric-sized cardiac rings were created and characterized for cell viability, distribution, and function. I studied the electrophysiological and structural maturation of cardiomyocytes within these cardiac rings after mechanical stimulation, electrical stimulation, and combined electromechanical stimulation in a bioreactor custom-made for these cardiac rings. Altogether, we showed improved electrophysiological maturation

using the combined factors of a dECM bioscaffold with electrical and mechanical stimulation.

DEDICATION

I dedicate this dissertation to my parents who have provided countless opportunities for me and supported me in all my academic and personal endeavors. Thank you for praying for me throughout my life, especially during the completion of this dissertation.

ACKNOWLEDGEMENTS

I would like to thank my committee chair, Dr. Ken Muneoka, my committee co-chair, Dr. Doris A. Taylor, and my committee members, Dr. John Criscione, and Dr. Robert Burghardt, for their guidance and support through the course of this research.

Thanks also go to the Texas Heart Institute Regenerative Medicine Research team for training me and discussing the results with me. I especially want to recognize Dr. Yutao Xi, Dr. Camila Hochman-Mendez, and Dr. Fernanda Mesquite for their exceptional help in my development as a student and scientist.

Finally, thanks to my family and friends for their encouragement, love, and prayers throughout my doctoral studies. A special thanks to my fiancé Nik Ong who has held me steady through the ups and downs of this dissertation and played a significant role in helping me achieve my doctoral degree.

NOMENCLATURE

CHAPS	3-((3-cholamidopropyl) dimethylammonio)-1-propanesulfonate
CM	Cardiomyocyte
Decell	Decellularization
dECM	Decellularized extracellular matrix
DIW	Deionized water
DW	Distilled water
EC	Endothelial cell
ECM	Extracellular matrix
EDTA	Ethylenediaminetetraacetic acid
GAG	Glycosaminoglycan
hiPSC	Human induced pluripotent stem cell
hiPSC-CM	Human induced pluripotent stem cell-derived cardiomyocyte
LV	Left ventricle
OGP	Octyl β-D-glucopyranoside
PBS	Phosphate buffered saline
RAEC	Rat aortic endothelial cell
Recell	Recellularization
SDC	Sodium deoxycholate
SDS	Sodium dodecyl sulfate

CONTRIBUTORS AND FUNDING SOURCES

Contributors

This work was supervised by a dissertation committee consisting of Professor Ken Muneoka [chair] and Professor Doris A. Taylor [co-chair] of the Department of Veterinary Physiology and Pharmacology, Professor Robert C. Burghardt of the Department of Veterinary Integrative Biosciences, and Professor John C. Criscione of the Department of Biomedical Engineering.

Parts of the introduction and literature review were written jointly with Nicole Mehta of the Department of Veterinary Integrative Biosciences and were published in 2018.

All other work conducted for the dissertation was completed by the student independently.

Funding Sources

Graduate study was supported by the Graduate Diversity Fellowship from Texas A&M University, the National Science Graduate Research Fellowship under Grant No. DGE-1252521, the Center for Cell and Organ Biotechnology, and the Texas Heart Institute. Parts of this research work were supported by the DARPA Program Office under Contract No. W31P4Q-16-C-0096.

The contents of this work are solely the responsibility of the authors. Any opinion, findings, and conclusions or recommendations expressed in this material are those of the author and do not necessarily reflect the views of Texas A&M University, the National

Science Foundation, the Center for Cell and Organ Biotechnology, the Texas Heart Institute, or the DARPA Program Office.

TABLE OF CONTENTS

Page

LIST OF FIGURES

Page

LIST OF TABLES

Page

1. INTRODUCTION AND LITERATURE REVIEW*

1.1. Problem Statement

Cardiovascular disease continues to be the leading cause of death worldwide, with more patients progressing to heart failure each year.[1-3] Current treatments for heart failure are targeted at symptomatic improvements whereas newer investigative strategies are aimed at repairing injured myocardium or regenerating healthy myocardium, often via regenerative medicine approaches. Despite recent advancements in the field, few patients regain full cardiac function. Currently, the most effective treatment for patients with end-stage heart failure is cardiac allo-transplantation.[4,5] However, the list of patients awaiting transplant far exceeds donor hearts available.[6] Therefore, developing alternative treatments for heart failure remains a top priority.[7]

1.2. Cardiovascular Tissue Engineering

One potential alternative to donor-dependent heart transplants is engineering bioartificial hearts. The field of tissue engineering was first defined in 1988 as the "application of principles and methods of engineering and life sciences toward fundamental understanding of structure-function relationship in normal and pathological mammalian tissues and the development of biological substitutes to restore, maintain, or

*Part of this chapter and tables are reprinted with permission from Cardiac Extracellular Matrix, edited by Eric G. Schmuck, Peiman Hematti, Amish N. Raval, 2018, Springer Nature, Switzerland. Copyright 2018 by Springer Nature Switzerland AG. DOI: https://doi.org/10.1007/978-3-319-97421-7_5

improve functions."[8] In the field of cardiovascular tissue engineering, physicians, scientists, and engineers seek to use the right combination of scaffolds, cells, and signals to create native-like tissue for drug testing, disease modeling, and organ repair and regeneration.[9,10] The following sections will focus on the scaffolds, cells, and biophysical signals studied in dissertation research.

1.2.1. Scaffold

Scaffolds replace or support damaged cardiac tissue by providing support and creating a structure for cells. An acellular scaffold could be applied to the surface of the heart to prevent, or even reverse, dilatation, or could be dosed with cells and delivered at the site of injury to aid in the restoration of lost cardiac cells and promote healing. Ideal scaffold candidates should be compatible with all cell types found in the heart, provide mechanical strength as location demands, guide cells to organize properly, and deliver biochemical cues for appropriate cell function within the heart.[11] These scaffolds may be sourced from biologic or synthetic materials, each of which has advantages and disadvantages. Synthetic materials are not always biodegradable and often lack the characteristics required for vascular and parenchymal cell attachment and infiltration,[12] but can easily be crafted into virtually any size or shape. In contrast, biologic scaffolds – typically derived from extracellular matrix (ECM) – retain biological cues necessary for cell migration, alignment, and differentiation but can be difficult to obtain in a sterile reproducible fashion and generally have low mechanical strength for cardiovascular application. The focus of this dissertation research is biologic scaffolds derived from

whole hearts, typically via removal of cells, to yield the cardiac extracellular matrix (ECM).

1.2.1.1. Decellularization

Decellularization of heart is carried out by chemical,[13-16] enzymatic,[17-19] or physical[20] means with varying degrees of cell removal.[21] Chemical-based decellularization changes osmotic gradients to initiate cell membrane lysis and removal. Enzymatic decellularization cleaves cell membranes, cell-cell attachments, cell-ECM attachments, or nucleic acid ECM attachments with specific enzymes to remove cells or cell remnants from the organ. Physical methods of decellularization use techniques such as tissue freeze-thawing cycles to lyse cell membranes. Each of these is followed by a cell debris washout either via immersion or perfusion. Immersion involves the submersion of the organ, with or without agitation and then repeated solution changes to remove cellular debris. It can be viewed as an outside-in wash. Perfusion-based decellularization was developed in the Taylor lab.[13] It is solution-agnostic, takes advantage of the native vasculature or other tissue conduits, and is the method of choice for solid, whole organs.[13,21,22] In the heart, perfusion is often performed via the aorta in a fashion that allows full perfusion through the coronary tree.

With any method of decellularization, the primary goal remains preservation of the native ECM composition, stiffness, and overall structure. However, each method of decellularization disrupts the ECM to varying degrees, and care must be taken to minimize ECM damage, while also eliminating cellular content. The standard for determining complete decellularization has been established as: 1) less than 50 ng of double stranded

DNA (dsDNA) per mg dry weight of ECM, 2) less than 200 base pair DNA length, and 3) no nuclei visible upon staining using either hematoxylin and eosin (H&E) or DAPI (4',6-diamidino-2-phenylindole) staining.[23,24] A summary of decellularization techniques is covered in Table 1.

1.2.1.2. Recellularization

Recellularization involves the seeding of vascular, parenchymal, and support cells into a previously decellularized scaffold. Parameters important for recellularizing the heart include cell type, cell concentrations, and seeding strategies. The variable cell composition within the heart presents a challenge when establishing the ratio of each cell type needed to recellularize the scaffold.[37-39] Research groups have recellularized murine and porcine hearts with murine or human cells, and a handful of labs have published results from human hearts recellularized with human cells.[14,40] These reports employed different recellularization techniques: perfusion, direct injection, and a combination of perfusion and direct injection. This section discusses each recellularization strategy and its application in engineering whole cardiac tissue from decellularized ECM (dECM). A summary of the recellularization techniques covered can be found in Table 2.

Table 1 Summary of decellularization techniques used for whole cardiac tissues. Reprinted with permission from Springer Nature Switzerland AG, Copyright 2018.

Decellularization Method	Species	Perfusion Technique through Cardiac Vasculature	Decellularization Protocol Used	Sterilization	Advantages/Disadvantages	Outcomes	Reference
Chemical	Rat	Ascending aorta	Compared 3 perfusion protocols: 1% SDS, 1% PEG, 1% Triton X-100	Pen/strep with amphotericin B -124 hrs	SDS gave improved DNA results; yielded fully decellularized construct over 12 hours with minimal matrix alterations	SDS perfusion for over 12 hours gave fully decellularized constructs- when used with Triton x-100, there was almost no detectable residual SDS levels	Ott et al.[13]
	Murine	Aorta	1% SDS overnight, Triton X-100 1 hr	Pen/strep - 72 hrs	IHC confirmed low DNA content; no DNA data to support conclusion	GAG/collagen structure was retained, could decellularize heart in ~24 hours	Ng et al.[25]
	Rat	Aorta	1% SDS overnight, 1% Triton X-100	Pen/strep in PBS		Successfully decellularized rat hearts with low DNA content	Robertson et al.[21]
	Porcine	Aorta, 100 mmHg	Heart was immersed in PBS solution. 4% SDS for 12 hrs, PBS rinse steps every 3 hrs.	Pen/strep - 24 hrs	GAG/ Collagen/ Elastin content remained high. Higher DNA content than acceptable range (82.6 +/- 3.2 ng DNA/mg tissue)	Successfully decellularized the porcine heart with high residual DNA content~17.45%	Weymann et al.[26]
	Human	Aorta, 80-100 mmHg	1% SDS for 4 days, then rinsed with PBS. Finished with 20 L of water	Pen/strep		Successfully decellularized the human heart, with only 5% residual DNA	Sanchez et al. [27]

Table 1 Continued

Decellularization Method	Species	Perfusion Technique through Cardiac Vasculature	Decellularization Protocol Used	Sterilization	Advantages/Disadvantages	Outcomes	Reference
Chemical	Human	Aorta, 60 mmHg	Perfusion with 1% SDS- 168 hrs, DIW 24 hrs, 1% Triton X-100 24 hrs, Final PBS wash for 168 hrs	Antibiotics and Antifungal solutions	Decellularized matrices contained high amounts of collagens, GAGs, laminins, and fibrillins.	Could decellularize human hearts with only 0.95% DNA content remaining	Guyette et al.[28]
	Porcine	Aorta, 4-5 PSI	Perfusion with 1x PBS - 1 hr, DW - 1 hr, 5% SDS - 1 hr, DW - 1 hr •Repeat with SDS - 2 hrs and DW for 2 cycles; SDS - 3 hrs and DW- 4 hrs •Perfused with 1% Triton X-100 - 2 hrs	None noted	Finished entire protocol in 24 hours, however GAG, Collagen, and ECM concentrations not reported	Could complete decellularization of whole porcine heart with 98% DNA removal and only 6 hours of exposure to detergents	Hodgson et al.[15]
	Porcine	Aorta	4 different experimental groups: 1. 3% SDS, 3% Triton X-100- 70-80 mmHg 2. 3% SDS, 3% Triton X-100- 90 mmHg 3. 3% SDS, 3% Triton X-100, 10% CHAPS, 1% OGP- 120 mmHg 4. 3% SDS, 3% Triton X-100, 1% OGP, 10% CHAPS-140 mmHg	None noted	Protocol 2 was found to be optimal. Protocol 1 did not complete decellularization in 5 days due to low pressures. Protocol 3 and 4 did not have complete decellularization, and pressure was so high that the matrix did not resemble native tissue	Final decellularization protocol: 3% SDS - 12 hrs, water rinse, 3% SDS - 24 hrs, water rinse, 3% Triton X-100 rinse - 24 hrs, water rinse, and PBS rinses at 90 mmHg	Ferng et al.[29]

Table 1 Continued

Decellularization Method	Species	Perfusion Technique through Cardiac Vasculature	Decellularization Protocol Used	Sterilization	Advantages/Disadvantages	Outcomes	Reference
Chemical and Enzymatic	Murine	Aorta	Frozen at -80ºC •Rinsed with 0.02% Trypsin, 0.05% EDTA, 0.05% NaN3 - 20 min •1% SDS, 0.05% NaN3 -10 min •3% Triton X-100, 0.05% EDTA 0.05% NaN3 - 10 min •4% DCA - 5-10 min	0.1% peracetic acid and 4% Ethanol for 5 minutes	Decreased the DNA content to be 3% residual DNA	Could decellularize murine hearts successfully, proved that DNA could be detected accurately with histologic evaluation.	Lu et al.[30]
Chemical and Physical	Rat	Aorta, 75-80 mmHg	•1% SDS, 1% DCA, 0.05% Sodium azide -12 hrs • 20% glycerol, 0.05% sodium azide, 25 mM EDTA in 0.9% NaCl -12 hrs •1% saponin and 0.05% sodium azide - 12 hrs • 20% glycerol, 0.05% sodium azide, 25 mM EDTA in 0.9% NaCl -12 hrs •200 IU/ml DNase I with MgCl - 12 hours	Pen/strep - 12 hrs storage: in PBS in pen/strep	Made a whole heart bioreactor to automate the whole heart decellularization and recellularization process; could successfully decellularize rat hearts with no contamination.	Reported low DNA results and some preliminary recell success	Hulsmann et al.[31], Aubin et al.[32]

Table 1 Continued

Decellularization Method	Species	Perfusion Technique through Cardiac Vasculature	Decellularization Protocol Used	Sterilization	Advantages/Disadvantages	Outcomes	Reference
Chemical and Physical	Porcine	Aorta and pulmonary artery	Repeated 8 times in this order - 4% SDS, agitation with SDS, 1% Triton X-100, perfusion with Triton X-100	0.1% peracetic acid and sterile PBS Storage: in antibiotics and antifungal solutions	Low DNA content achieved, GAG content decreased in LV	Decellularized the whole porcine heart, but GAG content in LV was significantly damaged	Methe et al.[33]
	Porcine	Aorta, 3-5 PSI	Alternating cycles of 1x PBS - 1 hr, water •3 Cycles of: 0.5% SDS - 2 hr, DW - 2 hrs •Rinsed with H2O - 2 hrs (nonrecirculating), then recirculating H2O -12 hrs •Perfused with 1% Triton X-100 - 2 hrs	None noted	GAG content was significantly reduced in the RA and RV, but remained similar to native in LV and LA. Collagen contents were similar throughout the heart	Reported 99-97% DNA removal in different areas	Momtahan et al.[34]
	Porcine	Ascending aorta, 100 mmHg	Frozen at -80ºC for 24 hrs, followed by 1% SDS, 1% Triton	None noted	Did not quantify DNA/gag/collagen content	Saw no DNA staining with DAPI after 12 hours	Kitahara et al.[16]

Table 1 Continued

Decellularization Method	Species	Perfusion Technique through Cardiac Vasculature	Decellularization Protocol Used	Sterilization	Advantages/Disadvantages	Outcomes	Reference
Chemical and Physical	Porcine	1. Upright hearts: descending aorta 2. Vented hearts: BA with hole in LV and cannula 3. Inverted orientation of hearts: DA at 45º angle upside down- 60 mmHg	•500 mM NaCl rinse - 4 hrs •20 mM NaCl rinse -2 hrs •1% SDS perfusion - 60 hrs •Final PBS wash	None noted, did not recellularize scaffolds	Inverted orientation of heart had lowest DNA content ~7%, and could achieve this within 3 days without compromising GAG/collagen content	Improved aortic valve conditions with inverted perfusion orientation, better coronary perfusion, and heart shape retention.	Lee et al.[22]
Chemical, Enzymatic, Physical	Porcine	Aorta	Froze hearts at -80ºC - 24 hrs • 0.2% Trypsin, 0.05% EDTA, 0.05% NaN3 at 37C - 3 hrs •Water followed by 2x PBS perfusion •3% Triton X-100, 0.05% EDTA, 0.05% NaN3 - 2.5 hr room temp •4% SDC - 3 hrs	0.1% peracetic acid/ 4% ethanol solution for 1.5 hours at 2,200 ml/min	Higher than acceptable DNA content in RV~ 55 ng DNA/mg tissue	Fast perfusion protocol and low DNA in LV, but higher than acceptable DNA in RV.	Remlinger et al.[35]

Table 1 Continued

Decellularization Method	Species	Perfusion Technique through Cardiac Vasculature	Decellularization Protocol Used	Sterilization	Advantages/Disadvantages	Outcomes	Reference
	Porcine	Aorta	Froze at -80ºC for 24 hrs in 4 solutions: 1. 0.02% Trypsin 0.05% EDTA, 0.05% NaN3 - **7 days** 2. 0.02% Trypsin 0.05% EDTA, 0.05% NaN3 - **1 day,** and 3% Triton x-100, 0.05% EDTA 0.05% NaN3 - **6 days** 3. 2. 0.02% Trypsin 0.05% EDTA, 0.05% NaN3 - **3 days**, and 3% Triton x-100, 0.05% EDTA 0.05% NaN3 - **4 days** 4. 3% Triton x-100, 0.05% EDTA 0.05% NaN3 - **7 days**	None Noted	Triton only treatment caused a 40% decrease in collagen content and 30% decrease in elastin; but had high residual DNA.	Trypsin only removed 59% DNA, while Triton only removed 40% DNA. The combination of protocol 2 and 3 resulted in a decrease of 90% and 91% respectively	Merna et al.[36]

Abbreviations Used: SDS- Sodium Dodecyl Sulfate, PBS- Phosphate Buffered Saline, Hrs- Hours, DIW- Deionized water, DW- Distilled water, min- minutes, CHAPS-(3-((3-cholamidopropyl) dimethylammonio)-1-propanesulfonate), OGP-Octyl β-D-glucopyranoside, EDTA-Ethylenediaminetetraacetic acid, DCA-Deoxycholic acid, SDC- Sodium Deoxycholate , BA- Brachiocephalic artery, DA, Descending Aorta, LV-Left ventricle, RV-Right ventricle, GAG- Glycosaminoglycan

Table 2 Summary of recellularization techniques used for decellularized whole cardiac tissues. Reprinted with permission from Springer Nature Switzerland AG, Copyright 2018.

Recellularization Method	Species from which the cardiac bioscaffold was derived	Cell Type	Cell Number	Culture Conditions	Cell Washout	Observations	Reference
Manual injection	Mouse	hESC and hMEC	3 million	Static culture for 14 days	Injection of cells was monitored by loss of cells from decellularized heart	Embryonic stem cells and progenitor cells expressed cardiac specific markers after 14 days in vitro culture and after in vivo subcutaneous transplantation.	Ng et al.[25]
Retrograde coronary perfusion via aorta	Mouse	Day 6 EBs	10 million	No continuous perfusion in first 5 days. 30 min media perfusion every 8 hours.	~10-15% repopulated cells preserved after 7 days perfusion	New method of periodic perfusion method saved time, medium, and avoided contaminations during 14-16 days of perfusion. Periodic perfusion method could consistently make beating heart constructs.	Lu et al.[30]

Table 2 Continued

Recellularization Method	Species from which the cardiac bioscaffold was derived	Cell Type	Cell Number	Culture Conditions	Cell Washout	Observations	Reference
Aortic infusion	Rat	rat aortic ECs	20 million	7 days of continuous perfusion via aorta with flow rate progressively increased from 1 to 3 ml/min over 3 days.	Not measured	All infusion methods were effective in delivering cells into the dECM bioscaffold. Combination of IVC and BA infusion of ECs improved distribution of cells in the mid-ventricular free wall vessels. Re-endothelialization before recellularization with neonatal cardiac cells improved contractility in vitro.	Robertson et al.[21]
BA infusion			20 million				
BA infusion			40 million				
IVC and BA infusion			20 million IVC, 20 million BA				

Table 2 Continued

Recellularization Method	Species from which the cardiac bioscaffold was derived	Cell Type	Cell Number	Culture Conditions	Cell Washout	Observations	Reference
5 injections in anterior left ventricle with 27-G needle	Rat	rat neonatal CM, fibrocytes, EC, and smooth muscle cells	50-75 million	Injections performed during retrograde perfusion. No electrical stimulation in first 24 hr, then 10-ms pulse of 5V through epicardial leads.	46% of cells lost within 20 min	Day 8: electric and contractile responses to single paces. Average recellularization was 33.8% proximally to injection sites. Areas of confluent cellularity was approximately 1 mm thick. Viability was >95% throughout thickness (0.5-1.1 mm).	Ott et al.[13]
Direct infusion into patent aorta		rat aortic EC	20 million	45 min static period for attachment, then 1 week of perfusion	Not measured	Day 7: Average cellularity was 550.7 endothelial cells per mm^2 on endocardial surface and 264.8 ECs per mm^2 within vascular tree.	

Table 2 Continued

Recellularization Method	Species from which the cardiac bioscaffold was derived	Cell Type	Cell Number	Culture Conditions	Cell Washout	Observations	Reference
Injected via cannula and directly through myocardium with an 18-gauge needle	Rat	Canine blood outgrowth EC	20 million	Static culture for 45 min before partially submerged in 500 ml of recirculating media.	Not measured	Widespread adhesion of seeded cells following 9 days of culture. Observations: clusters of cells consistent with proliferation during culture; substantial cell spreading and multiple focal adhesions.	Crawford et al.[41]
Aortic infusion	Porcine	HUVEC passage 2-6	5-6 million	12-14 days with electrodes pacing on left midventricular wall. 3 weeks of perfusion time.	Not measured	Day 10: Average recellularization per cross-section of scaffold was >50% around injection sites. MEA demonstrated discrete foci with electric voltage undulations of up to 200 mV in time scale of ~500-1000ms.	Weymann et al.[26]
5 intramural injections (8-10mm depth) in anterior left ventricle with a 27-G needle		rat neonatal CM	8-9 million		Not measured		

Table 2 Continued

Recellularization Method	Species from which the cardiac bioscaffold was derived	Cell Type	Cell Number	Culture Conditions	Cell Washout	Observations	Reference
10 segments of 0.1ml suspension injected in left ventricular wall	Rat	murine myoblast cell-line (C2C12)	1 million/ml (100k/0.1 ml)	After 24 hours of seeding, 96 hours with biomechanical conditioning: 10% longitudinal elongation of ECM	Not measured	Increased cellular viability was reported after 72 hours of cultivation of pre-seeded scaffolds under stimulated vs. non-stimulated conditions.	Hulsmann et al.[31]
5 Intramyocardial injections	Human	BJ RiPS-derived cardiomyocytes	500 million	Static culture for 3-4 hours, then perfusion culture started at 20 ml/min for 12 hours, then 60 ml/min on day 2.	Mattress sutures tied at each injection point before needle extraction to minimize cell loss.	Dense regions of engrafted iPS-CM in left ventricular wall; tissue repopulation of <50% within target region of 5 cm^3. Coronary perfusion maintained >90% viability after 14 days in culture.	Guyette et al.[28]

Table 2 Continued

Recellularization Method	Species from which the cardiac bioscaffold was derived	Cell Type	Cell Number	Culture Conditions	Cell Washout	Observations	Reference
Antegrade coronary perfusion	Rat	rat neonatal CM, fibroblasts, EC	100 million	Continuous perfusion in 5% CO_2 atmosphere. Medium changed at day 2 or 3 and then every 48-72 hours following.	Not measured.	Spontaneous contractions at days 2-30. Unsynchronized and well-synchronized beating was observed.	Yasui et al.[42]

Abbreviations Used: EC - Endothelial cells; CM - cardiomyocyte; hESC - human embryonic stem cell; hMEC - human mammary epithelial cell; EBs - Embryoid bodies; iPS - induced pluripotent stem cell; IVC - inferior vena cava; BA - brachiocephalic artery;

1.2.1.2.1. Direct Injection

The direct injection of cells into the heart involves using a syringe and needle to inject cells suspended in media into the area of interest. The use of a needle presents a concern that the ECM is damaged during the injection process. Additionally, since cells are injected into one specific location, and migration is often limited, cell density is not uniform throughout the ECM. In the first published study of a recellularized human heart, 500 million cardiomyocytes derived from human BJ fibroblast RNA-induced pluripotent stem cells (BJ RiPS) were injected using five intramyocardial direct injections between the left anterior descending artery and the left circumflex artery.[14] Upon histological analysis after two weeks, the 5 cm3 injection region of the tissue showed approximately 50% cell repopulation, confirming that uniform cell density is still lacking after recellularization via direct injection.[14]

A shortcoming of recellularizing a scaffold via direct injection is the loss of cells during the injection, contributing to low numbers of cells observed in the parenchyma of the cardiac dECM bioscaffold in various studies.[14,16,31] Steps can be taken to mitigate the loss of cells, such as adding sutures to the sites of injection, as was done in the recellularization of the human heart; however, full cellularity of the parenchyma was still not achieved in this study. As functional cardiac tissue requires enough viable cells for gap junction formation and cardiomyocyte contractility in the parenchyma, it is critical to have complete cellular coverage in the recellularized heart. Research is ongoing to develop improved injection techniques for complete cell coverage of whole heart bioscaffolds.

1.2.1.2.2. Perfusion

Perfusion-based recellularization utilizes the native vascular conduits in the heart as a pathway to deliver cells. Perfusion-based recellularization is accomplished by cannulating one of the major vessels leading to the heart, most often the aorta, which allows for access to coronary arteries. Perfusion usually involves two steps: delivery of the cells where flow occurs, followed by a period of "rest" to allow cells to adhere. The adhesion of cells to the matrix is critical in all recellularization protocols but is particularly important when perfusion occurs shortly after delivery. If cells are not allowed sufficient time or provided sufficient conditions to adhere to the ECM, cells will be "washed out" of the ECM during reperfusion, and incomplete recellularization will occur. This loss of cells would therefore result in a need for larger cell numbers for any recellularization process.

In 2011, Ng et al. cannulated the aorta of a decellularized mouse heart to deliver human embryonic stem cells (hESCs) and human mesendodermal-cells derived from hESCs to the vasculature of the heart via perfusion.[25] After the heart was in static culture for 14 days, researchers found that the stem cells expressed endothelial cell (EC) markers in the vasculature, suggesting that site-specific cues were retained in the matrix and contributed to progenitor cell differentiation. In a similar manner, Lu et al. repopulated murine hearts with cells from an embryoid body, via retrograde coronary perfusion.[30] Cells then differentiated within the recellularized dECM into cardiomyocytes and smooth muscle cells (SMCs), resulting in spontaneous contractions, new vessel formation, and responsiveness to isoproterenol, a beta-adrenergic agonist, and E4031, an antiarrhythmic agent. Although contraction occurred, evidence of arrhythmias suggested the cells were

immature and that gap junction formation between cardiomyocytes was incomplete. These studies provided further confirmation that the coronary vascular tree is intact after decellularization and can be used to deliver cells to various areas of the matrix.

Due to the unidirectional flow, perfusion recellularization can result in higher cell density in large vessels that are proximal to the infusion site – upstream of smaller vessels. Yasui et al. perfused a mixture of 100 million cardiomyocytes, fibroblasts, and ECs antegrade through the coronary tree of a decellularized rat heart.[43] The variety of cells seeded into the matrix resulted in a non-homogeneous distribution of cells, with a higher concentration of cells found closer to large vessels and near well-perfused vascular beds. However, spontaneous contractions of the heart started 2-3 days after recellularization and continued for the length of the 30-day culture period, suggesting that although cell distribution was uneven, enough cellularity was achieved through perfusion to allow the partial formation of gap junctions.

To compare injection and perfusion side-by-side, Kitahara et al. recellularized one group of porcine dECM bioscaffolds by injection and a second group by perfusion, using 1.5×10^7 porcine mesenchymal stem cells (pMSCs) in each.[16] Recellularized hearts were then heterotopically transplanted into recipient pigs. The perfusion-recellularized heart did not show patent coronary arteries during intraoperative coronary angiography, as was observed in the scaffold recellularized by injection. Interestingly, none of the perfused cells were observed in vessel lumens upon scaffold excision, while thrombi and inflammatory cells were evident in the parenchyma. Cells already present vs. those recruited into the parenchyma were not separately identified in the study. The injected

pMSCs were seen in the parenchymal space in clusters and not homogeneously distributed. This observation confirmed that both methods could be used to revascularize and reseed portions of the cardiac dECM bioscaffolds, but both result in non-uniform distribution of cells throughout the matrix when compared directly.

1.2.1.2.3. Perfusion and Injection

Perfusion and injection is a combined approach to recellularizing the whole heart, delivering cells both with a needle into the parenchyma and to both parenchyma and vasculature via perfusion. Our lab routinely uses a combination of perfusion and intramyocardial injections to recellularize rat and pig hearts.[13,21] Previously, we established a closed-circuit retrograde perfusion system through the aorta to infuse rat aortic endothelial cells (RAECs) directly into the patent aorta of a decellularized rat heart.[13] Histological evaluation showed adhesion of RAECs on the endocardial surface and within the vasculature of the heart. When five injections containing a mixture of neonatal cardiomyocytes, fibrocytes, ECs, and smooth muscles cells were delivered into the anterior left ventricle, a high degree of cell retention at injections sites was observed (>80%), which led to cell coupling and electrical activity propagation. By day 8, the areas of confluent cellularity were about 1 mm thick, and throughout the thickness of the ventricular wall, cell viability was greater than 95%. Although a high density of cells was maintained near the injection sites, density decreased with distance from the needle track.

In another study by our group, rat hearts were re-endothelialized via three different methods: direct aortic perfusion of cells, perfusion of cells into the brachiocephalic artery (BA), or a combination of venous and arterial cell perfusions through the inferior vena

cava (IVC) and BA; the combination of venous and arterial perfusion resulted in enhanced distribution of endothelial cells within the vasculature. We found that re-endothelialization of the heart's vasculature by EC perfusion improved the contractility of cardiomyocytes injected into the myocardium.[21] This improved function is not surprising since endothelial cells have been previously shown to promote cardiomyocyte organization and survival.[44] Along with the method of delivery (injection or perfusion), the order in which cells are delivered into the matrix therefore plays a role in their survival and function.

Our findings of improved cell viability and contractility from a combination of perfusion and injection recellularization have been confirmed in the whole porcine heart as well. In a study by Weymann et al., 5-6 x 10^6 human umbilical vein endothelial cells (HUVECs) were first perfused through the aorta, and then five injections of 8-9 x 106 neonatal rat cardiomyocytes (NRCMs) were injected intramurally into the anterior left ventricle of the decellularized porcine heart.[26] The recellularized porcine hearts were found to have platelet endothelial cell adhesion molecule-1 (PECAM-1) positive cells in the large and small coronary arteries, with minimal gaps in cell coverage. The seeded cardiomyocytes exhibited intrinsic electrical activity after 10 days in culture, but average recellularization of the scaffold was 50% around the sites of cell injection, and significantly decreased farther away from the injection sites. The electrical activity of the injected cells, as measured by multi-electrode array, demonstrated that areas of functionality could be achieved in a large whole organ, but a larger number of cells may be necessary to get complete cell coverage.

To summarize, successful recellularization of decellularized cardiac bioscaffolds will require essentially recapitulating a native heart by replacing cells in the vasculature, parenchyma, valves, etc. This will require achieving uniform cell density in the parenchyma while also promoting vascularization. High cell numbers are required to achieve complete cell coverage, and this is especially true with larger human-sized hearts. While direct injection requires the insertion of a needle with a diameter large enough for cells to pass into the scaffold, this technique allows cells to be delivered to a specific location in the myocardium. Perfusion-based recellularization allows cells to reach almost every part of the heart by taking advantage of the native vasculature and cavities. Order of cell delivery is also important, as re-endothelialization of the vasculature prior to parenchymal recellularization increased retention of other cell types and improved function of the organ.[13,21] Additional studies are required for conclusive statements on the order of recellularization, especially if a progenitor cell type is delivered to whole cardiac bioscaffolds.

1.2.2. Cells

Once the bioscaffold has been chosen, we need to use the right combination of cell types to repopulate the bioscaffold. To create bioengineered tissue constructs with clinical potential, scientists have identified induced pluripotent stem cells (iPSCs) as a potential cell source, since they can be generated from adult somatic cells, can be expanded several orders of magnitude *in vitro*, and can be differentiated into multiple cell lineages, including cardiomyocytes (CMs).[45] The use of human iPSC-derived CMs (hiPSC-CMs) allows scientists to develop and screen therapies for patient-specific genetic diseases *in*

vitro[46] because hiPSC-CMs appear to retain disease phenotypes.[47,48] However, once differentiated into cardiomyocytes, hiPSC-CMs have a low proliferative capacity[49] and an immature cardiac phenotype.[50]

The immature phenotype of hiPSC-CMs includes electrophysiological[51-53] and structural[54,55] characteristics that suggest hiPSC-CMs exhibit a phenotype that lies between early fetal and adult CMs. While hiPSC-CMs display key properties such as cardiac-type action potentials and an excitation-contraction coupling mechanism that confirm their CM identity, other properties, such as calcium handling, conduction velocity, and contractile properties, do not reflect those observed in adult CMs. Since hiPSC-CMs are phenotypically comparable to immature CMs *in vivo*, some of the same factors that influence maturation in embryonic and fetal development may be used to promote hiPSC-CM maturation *in vitro*.[56] Enhancing hiPSC-CM maturation is critical to engineer physiologically accurate models of the adult heart, to perform disease-specific drug screens , and to repair damaged or diseased native myocardium.[57] In addition to using the bioscaffold as an environment to promote hiPSC-CM maturation, signals, the third component of tissue engineering, can be used.

1.2.3. Biophysical Stimulation

Investigators have used various signals such as growth factors, time, and biophysical stimulation to mature human CMs in vitro. Biophysical stimuli such as electrical activity and mechanical forces are present in the developing native heart, making them both excellent candidates for signaling CM maturation. Some initial studies using

electrical and mechanical stimulation in three-dimensional (3D) engineered tissue environments have already shown promising results.

1.2.3.1. Electrical Stimulation

Electrical activity has been used in tissue engineering because early studies showed the electrical pacing of 3D cardiac tissue constructs was found to be more physiologically relevant.[58] Cardiomyocytes that were cultured with only mechanical stimulation were found to have improved cell differentiation and force of contraction when compared with unstimulated culture cells; however, some characteristics of cardiomyocyte development were lacking, even in 3D culture systems. Thus, electrical stimulation in a 3D environment is thought to contribute to the maturation of cardiomyocytes. Evidence of cardiomyocyte maturation that has not yet been achieved include a visibly mature M band, an intercalated disk pattern and T-tubules.[59-61] Over the years, different 3D structures for heart tissue have arisen. One such 3D cardiac construct is biowire, in which cells are seeded onto a surgical suture in a collagen gel. After having undergone electrical field stimulation, the cells in the biowire showed cell alignment along the length of the wire, physiologic hypertrophy, and cell maturation through well-defined Z discs and myofibrils.[62] However, researchers are still in search of a culture or bioreactor system that will result in cardiomyocytes with evidence of terminal differentiation, such as T Tubules.[61] The absence of T-tubules can cause cardiomyocytes to display unsynchronized calcium transients, which reflect an immature state of cardiomyocytes.[63] As researchers expand their use of electrical stimulation in 3D constructs, further improvements are made upon the initiation, pacing, and duration of the electrical activity.

1.2.3.2. Mechanical Stimulation

Cardiomyocytes typically undergo two different biomechanical forces, stretch and perfusion. At lower frequencies, cyclical stretch lowered gene expression whereas higher frequency cyclical stretch increased gene expression over observations made in the unstretched controls.[64] Spontaneously contracting engineered heart tissue can be achieved through various culture conditions, including auxotonic loading. Twitch tension in response to calcium release increased in 3D loops of engineered heart tissue.[65] Even with the number of studies on mechanical stress in 3D culture systems, the heart's response to mechanical stimulation in the whole heart is not fully understood. In the recellularized heart, mechanical stimulation can be accomplished through balloon or perfusion.

1.2.3.2.1. Balloon

Hülsmann et al. inserted an inflatable latex balloon into the rat heart.[31] The balloon was filled with an incompressible fluid to vary the volume within the LV and transfer pressure-energy. Researchers could control the frequency at which volume-strokes were pulsated into the system. Induced expansion of the endoventricular cavity, and thereby stretch of the heart ECM, increased cellular viability and cellular 3D spatial orientation of the cardiomyocytes. Similarly, to how stretch aligns cardiomyocytes in 2D culture, the cells in the whole heart ECM had elongated cell bodies and formed aligned cellular networks within the matrix.

Guyette et al. also used a balloon to expand the ventricle of the human heart in a custom heart bioreactor.[14] The strain regimen began on day 7 of culture after cell delivery and continued to day 14 when electromechanical functional analysis took place.

1.2.3.2.2. Perfusion

Another method to induce stretch in the left ventricle is through medium perfusion. The flow of medium is adjusted to allow the heart's valves to close. Similar to how the balloon stretch could be controlled through stroke volume, the flow rate can be adjusted to determine frequency and stretch over time.

In the initial study that decellularized the whole heart through perfusion decellularization, the Taylor lab used pulsatile antegrade left heart perfusion and a circuit of coronary flow through the left atria to create a pressure gradient.[13] The pressures were then adjusted to allow closure of the aortic valves between each pulse. This aortic valve closure provides the pressure needed to have pulsatile coronary perfusion, as seen during diastole and ventricular relaxation of the human heart. The preload and afterload of the culture medium gave the investigators more control over the pulsatile LV distension so that a known amount of stretch can be applied through the fluid.

1.3. Conclusion

Altogether, the combination of cells, biophysical signals, and scaffolds used in cardiovascular tissue engineering need to be thoughtfully studied to improve the current state of cardiovascular tissue engineering. The interplay of dECM bioscaffolds, human cardiac cells, and biophysical signals in the form of electromechanical stimulation still need to be tested and understood. This dissertation aims to bring new insights and discoveries to the field of cardiovascular tissue engineering.

2. GELATIN PROMOTES CELL ADHESION AND SURVIVAL WITHIN DECELLULARIZED HEART EXTRACELLULAR MATRIX VASCULATURE AND PARENCHYMA

2.1. Synopsis

2.1.1. Introduction

Recellularization of an organ decellularized extracellular matrix (dECM) offers a potential solution for organ shortage in allograft transplantation. Cell retention rates have ranged from 10% to 54% in varying approaches for reseeding cells in whole organ dECM scaffolds. We aimed to improve recellularization by using gelatin as a cell carrier to deliver endothelial cells to the coronary vasculature and cardiomyocytes to the parenchyma in a whole decellularized heart.

2.1.2. Methods

Rat aortic endothelial cells (RAECs) were perfused over decellularized porcine aorta in low (1%) and high (5%) concentrations of gelatin to assess attachment to a vascular dECM model. After establishing RAEC viability and proliferation in 1% gelatin, we used 1% gelatin as a carrier to deliver endothelial cells and cardiomyocytes to decellularized adult rat hearts. Immediate cell retention in the matrix was quantified, and recellularized hearts were evaluated for visible contractions up to 35 days after recellularization.

2.1.3. Results

We demonstrated that gelatin increased RAEC attachment to decellularized porcine aorta; blocking integrin receptors reversed this effect. In the whole rat heart dECM scaffold, 1% gelatin increased both RAEC and neonatal rat cardiomyocyte (NRCM) retention immediately after cell infusion into coronary vasculature and injection into cardiac parenchyma, respectively, when compared with the control group without gelatin. Gelatin was associated with visible contractions of NRCMs within hearts (87% with gelatin versus 13% control).

2.1.4. Conclusions

Gelatin was an effective cell carrier for increasing cell retention and contraction in dECM, with the gelatin-cell-ECM interactions likely mediated by integrin.

2.2. Introduction

The number of new patients diagnosed with heart failure is increasing, especially as the population ages.[66,67] The definitive treatment for end-stage heart failure is heart transplantation;[68] however, the limited number of donor hearts prevents transplantation from having a large impact on the prevalence of heart failure. Thus, there is a significant need for new treatment options for this devastating disease.[69]

One approach to address the donor shortage is to create a bioartificial heart by reseeding a bioscaffold, such as a decellularized cadaveric heart, with human cells.[13,70,71] We proposed that approach a decade ago when we reported that we had decellularized and reseeded a cadaveric rat heart with neonatal rat cardiomyocytes (NRCMs).[13] However, adequate reseeding of a whole organ decellularized extracellular matrix (dECM) has been

challenging, whether the bioscaffold is rat,[13,42] pig,[42,72] or human[73] ECM. In some cases, as few as 10% to 15% of the cells have been preserved in the dECM after 7 days of perfusion with media and growth factors,[30] whereas other studies have shown cell retention rates of 10% to 54% in whole decellularized hearts.[13,30] These findings suggest that a major limitation in reseeding dECM is the large number of cells that do not attach to the scaffold but rather flow out of the heart. Other challenges of growing a bioartificial heart include generating the large number of cells needed for recellularization,[74,75] preventing blood coagulation,[76] and ensuring long-term graft viability[71]; however, none of these challenges can be addressed until viable cells can be delivered and retained in the scaffold.

We designed the current study to address the tissue engineering challenge of cell delivery and retention during recellularization of a cardiac dECM bioscaffold. We evaluated whether gelatin, a naturally derived protein, could be used as a cell carrier to increase endothelial cell and cardiomyocyte retention in a whole decellularized rat heart. We hypothesized gelatin would be a better cell carrier than medium for improving the retention of endothelial cells delivered to the dECM vascular tree and cardiomyocytes injected into dECM parenchyma.

2.3. Materials and Methods

2.3.1. Animal Experiments

All experiments were performed in accordance with the US Animal Welfare Act and were approved by the Institutional Animal Care and Use Committee at the Texas Heart Institute.

2.3.2. Rat Heart Harvest and Decellularization

Fischer rats (Charles River, Wilmington, MA) were anesthetized with 5% isofluorane and then heparinized with 1000 UI/ml sodium heparin intraperitoneally. The thoracic cavity was opened through a median sternotomy to expose the heart and its branching vessels. The brachiocephalic artery was ligated and cut. The aorta, superior vena cava, inferior vena cava, left pulmonary artery, and pulmonary veins were cut to remove the heart. The aorta was cannulated with a 1-mm cannula, and the heart was flushed with phosphate-buffered saline (PBS). Decellularization was modified from the previously described protocol.[13] Hypertonic (500 mM NaCl), hypotonic (20 mM NaCl), and 1% sodium dodecyl sulfate (SDS) solutions were perfused sequentially through an aortic cannula at a constant pressure of 70 mmHg for 10, 10, and 30 hours, respectively. Lastly, PBS was perfused at a flow rate of 5 ml/min for 24 hours. The decellularized hearts were stored in PBS at 4oC for recellularization at a later timepoint.

2.3.3. Porcine Aorta Decellularization

We obtained the ascending aorta from euthanized pigs. The aorta was cannulated at both ends and anchored at 45° with 10% of pre-stretch. Decellularization was achieved by sequentially perfusing hypertonic, hypotonic, and ionic detergent solutions through the aorta at 120 mmHg constant pressure; the perfusion was driven by a peristaltic pump controlled by a proportional-integral-derivative controller (Harvard Apparatus, USA). The following solutions were perfused sequentially over 72 hours: hypertonic (500 mM) NaCl for 4 hours, hypotonic (20 mM) NaCl for 2 hours, 1% SDS for 60 hours, and PBS for 6 hours. Decellularization was confirmed as previously described.[22]

2.3.4. Rat Aortic Endothelial Cell Culture

Commercially available rat aortic endothelial cells (RAECs, Cell Application, Inc., USA) were cultured in rat endothelial cell growth medium (Cell Application, Inc., USA) supplemented with 1% penicillin/streptomycin (Sigma-Aldrich, USA) and 10% fetal bovine serum. The culture medium was changed 3 times per week. RAECs were cultured at 5,000 cells per cm^2 in T-75 flasks according to manufacturer's instructions and kept below 8 passages before the experiments.[77] For in vitro experiments with gelatin, RAECs were trypsinized and resuspended in 1% or 5% porcine skin gelatin (w/w, Sigma-Aldrich) that was dissolved in medium.

2.3.5. Cell Attachment Under Laminar Flow *In Vitro*

After decellularization, the porcine aorta was dissected longitudinally and flattened to evaluate cell attachment to its surface under laminar flow. A sticky-slide flow chamber was mounted on the decellularized aortic luminal surface to form 6 channels that were 0.4 mm high and 17 mm long. RAECs were labeled with 1,1'-dioctadecyl-6,6'-di(4-sulfophenyl)-3,3,3',3'-tetramethylindocarbocyanine (SP-DilC18(3), Thermo Fisher Scientific, USA) and suspended in standard medium without any gelatin (control) and in media with low (1%) and high (5%) gelatin concentrations. Cell suspensions were infused through the laminar flow chamber at 1 ml/min for 3 minutes using a syringe pump (Harvard Apparatus) at room temperature. After the flow was stopped, the aorta was removed from the flow chamber, and the cells were fixed in 4% paraformaldehyde in situ for 20 minutes. When the experiment was repeated, a subset of cells was incubated with an antibody to block integrin α5β1 (anti-integrin α5β1 antibody, clone JBS5, Millipore,

USA)[78] for 1 hour to determine if integrin contributed to cell attachment to the aorta dECM in 1% gelatin. We obtained images of the cells attached to the aortic luminal surface by using a fluorescent microscope (Nikon, Japan) and counted attached cells per high-power field by using ImageJ software (NIH Image, National Institutes of Health, USA).

2.3.6. Cell Viability and Proliferation *In Vitro*

Cell viability and proliferation were quantified 7 days after seeding RAECs on tissue culture plates and culturing the cells in medium with different concentrations of gelatin (0%, 1%, and 5%). To assess cell viability, we used cell-permeant glycyl-phenyl-alanyl-aminofluorocoumarin (GF-AFC) (Promega BioSciences, USA), according to the manufacturers' instructions.[79] Cell proliferation was measured using a standard 3-(4, 5-dimethylthiazolyl-2)-2, 5-diphenyltetrazolium bromide (MTT) proliferation assay.[80]

2.3.7. Re-endothelialization of Decellularized Rat Heart

Before re-endothelialization, the aortic cannula was re-established and hearts were placed in PBS with penicillin (100 U/mL), streptomycin (100 μg/mL), and amphotericin B (2.5 μg/mL, Sigma-Aldrich, USA) at 37ºC for at least 8 hours, and then stabilized with medium at 37°C for at least 8 hours. On the basis of our results of cell viability, cell proliferation, and von Willebrand Factor (vWF) expression of RAECs in 1% and 5% gelatin, we used cells suspended in medium containing either no gelatin (control) or 1% gelatin for all ex vivo experiments. On the day of re-endothelialization, 40 million RAECs were trypsinized and suspended in 30 mL of medium containing 1% gelatin or medium only (control) at room temperature (20°C). The control and 1% gelatin cell solutions were infused through the cannula inserted into the aorta by using a syringe pump at 1 ml/min

for 30 minutes. During this infusion, the flow rate of medium through the left atrial cannula was 0.5

ml/min.[21] After RAEC infusion was complete, the flow through both cannulas was stopped for 1 hour to allow for cell attachment to the matrix. We collected the solution that perfused through the heart during cell infusion and counted the cells in the solution to quantify cell loss. The cell retention (cells infused minus cells lost) was expressed as a percentage of total cells infused. After the cell attachment period, the flow rate through the aortic cannula was set to 3 ml/min to supply oxygen and nutrients to the heart via coronary perfusion. The re-endothelialized heart was maintained at 37° for 7 days under constant flow in a Langendorff perfusion system (Harvard Apparatus), in which media was perfused through the aorta.

2.3.8. Viscosity of Whole Heart Perfusate

After the whole hearts were re-endothelialized, perfusate samples were collected every day for the first 5 days; after that, samples were collected whenever media in the whole heart was changed, which was approximately every other day. We measured the viscosity of the perfusate collected within the first 5 days by using an SV-10 viscometer (A&D Company, Japan).

2.3.9. Isolation and Preparation of Neonatal Rat Cardiomyocytes

Neonatal Sprague Dawley rats (1-3 days old) (Texas Animal Specialties, USA) were euthanized with an intraperitoneal injection of sodium pentobarbital (100 mg/kg) and heparin (150 mg/kg). The hearts were excised and immediately placed into PBS on ice. Then, the hearts were minced and placed into Hank's Balanced Salt Solution with trypsin

(10,000 U/mL, Sigma-Aldrich, MO) at 4°C overnight. Tissue pieces were digested in a solution of collagenase type II (200 U/mL) (Worthington Biochemical Co., USA) and 0.06% pancreatin (wt/wt, Sigma-Aldrich) in a Celstir (Wheaton, USA) at 37°C until no tissue remained, approximately 35 minutes. The digested cells were collected and passed through a 100-µm cell strainer. The cells were pre-plated in T-175 flasks and incubated for 1 hour to allow fibroblasts to attach to the flask. The supernatant was collected and plated for another hour to further reduce the number of fibroblasts. The final supernatant, which was enriched for NRCMs, was injected into decellularized hearts with or without gelatin.

2.3.10. Delivery of Neonatal Rat Cardiomyocytes to Re-endothelialized Rat Heart Extracellular Matrix

Seven days after decellularized rat hearts were re-endothelialized with RAECs, freshly isolated NRCMs were suspended either in 1% gelatin in medium or medium only at a final concentration of 100 million cells/ml. We used a 27-gauge needle to deliver the 1-ml cell solution (1% gelatin or control) in 5 separate injections spaced approximately 1-mm apart and parallel to the surface of the left ventricular free wall. The injection speed was set at 20 µl/min using a syringe pump (88-1050, Harvard Apparatus). Re-endothelialized hearts injected with NRCMs were cultured for 15 to 35 days paced with 2-ms long square waveform pulses of 10-15 volt at 1 Hz beginning at 1 day after addition of NRCMs (day 8).

2.3.11. Histology

At 15 to 35 days after re-endothelialization, recellularized rat hearts (with ECs and NRCMs) were sectioned into thirds from the base to the apex and fixed in 10% neutral buffered formalin at room temperature. The samples were dehydrated, embedded in paraffin, sectioned (6 μm), and placed on microscope slides for staining. After rehydration, slides from each of the 3 regions were stained with Masson's trichrome staining.[27] For immunofluorescence studies, slides were stained using an anti-integrin β1 antibody (Abcam, USA) and either anti-rat endothelial cell antigen marker (RECA1, Abcam) or cardiac troponin T (cTnT, Abcam) primary antibodies. Fluorescent-labeled secondary antibodies, goat anti-mouse IgG, Alexa Fluor 488 conjugate antibody, and goat anti-rabbit IgG, Alexa Fluor 488 conjugate antibody (Thermo Fisher Scientific), were used. Slides were then stained with 4′,6-diamidino-2-phenylindole (DAPI). The matrix was detected by using reflected light signals,[81] which enabled visualization of the autofluorescence of the ECM that originated primarily from collagen and elastin. Images were obtained with a Leica SP5 confocal microscope (Leica, Germany).

2.3.12. Statistical Analysis

All continuous variables (viability, fluorescence absorbance, cell number per square millimeter, and percentage of cells retained) were expressed as mean ± SEM. A Student *t* test was used for two-group comparisons. One-way ANOVA was used for comparing multiple concentrations of gelatin. A p-value less than 0.05 was considered significant. All data for statistical analysis were processed with Graph Pad Prism 5.0

(Graph Pad Software Inc., USA). Additional descriptions of the methods are available in the Supplementary Methods.

2.4. Results

2.4.1. Gelatin increased the attachment of Rat Aortic Endothelial Cells to Decellularized Aorta Surface under Laminar Flow

To test whether gelatin improved the attachment of RAECs to a biologically relevant substrate, we quantified cell attachment to the surface of a decellularized porcine aorta in a low (1%) and high concentration (5%) of gelatin. A fluid suspension of RAECs was perfused over decellularized aorta at a rate of 1 ml/min for 3 min, mimicking the minimum flow rate in the vasculature of a young person[82] (Figure 1A). Cell attachment to the aorta surface increased in the presence of gelatin in a concentration-dependent manner from 46.5 to 381.1 cells per square millimeter in 0 to 5% gelatin (Figure 1B and C, $p<0.001$, $n=11$ images analyzed). When an $\alpha5\beta1$ integrin-blocking antibody was incubated with the cells in 1% gelatin before the cell solution was perfused over the aorta, the number of RAECs that attached decreased to 40% of pre-incubation values ($p<0.05$) and was not significantly different from the number of RAECs attached when gelatin was not used ($p=0.54$; Figure 1C).

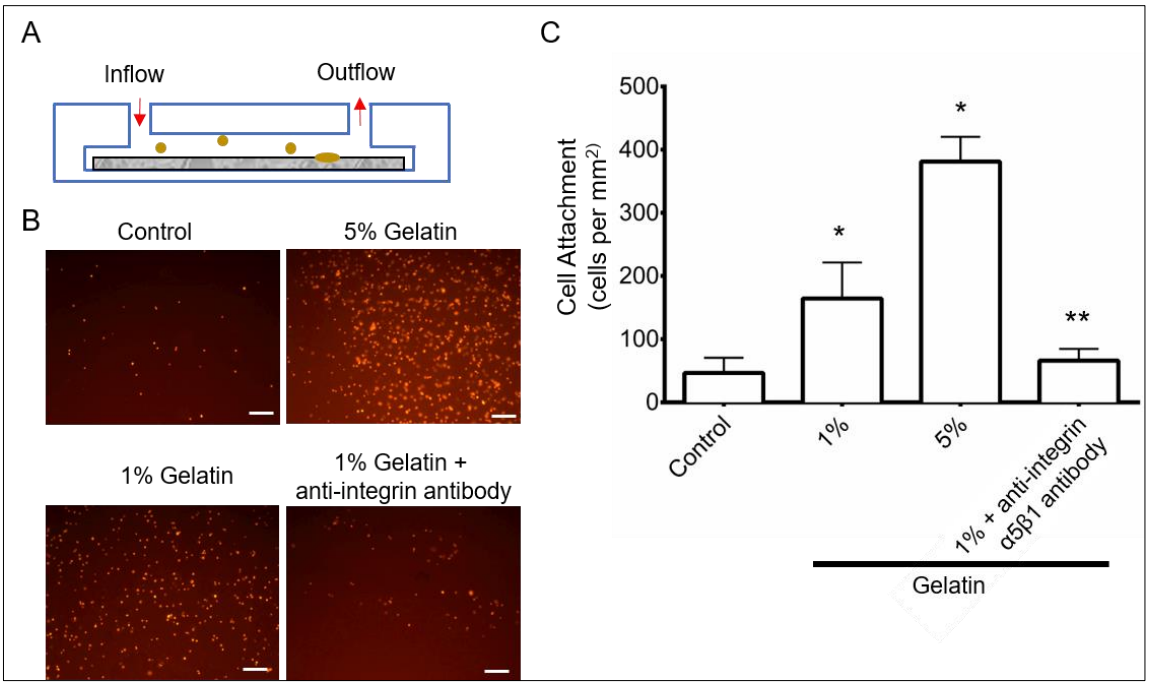

Figure 1 Gelatin increases cell attachment to decellularized porcine aorta under laminar flow.
A. Schematic figure showing the design of the in vitro laminar flow-through chamber. Red arrows indicate the direction of fluid flow over the decellularized porcine aorta, represented by the gray rectangle. Non-attached yellow cells are round when perfused over the aorta. Some cells attach to the matrix and spread out over time, as indicated by the yellow oval cell. B. Immunofluorescent images of cells attached to the vessel surface following 3 minutes of perfusion. Scale bar: 100 µm. C. Quantification of RAEC attachment to decellularized aorta. *p<0.001 vs Control; ** p<0.05 vs 1% Gelatin.

2.4.2. Gelatin Delayed Rat Aortic Endothelial Cell Attachment to Tissue Culture Plate In Vitro

Adding gelatin to cell culture medium during cell plating significantly delayed RAEC attachment to a standard tissue culture plate in a gelatin concentration-dependent manner; the experiments were conducted for 60 minutes at room temperature and for 120 minutes at 37°C (Figure 2). At room temperature, mixtures of 3% gelatin and higher

solidified into a gel before the first 15-minute time point and were not included in the cell attachment quantification studies. In general, cell attachment increased over time. In the control group (cultured in medium only), the number of cells attached to the culture plate increased until 45 minutes and decreased at 60 minutes, presumably due to cell death after being at room temperature for so long. For gelatin-exposed cells, the number of cells that attached decreased for each timepoint as the gelatin concentration increased.

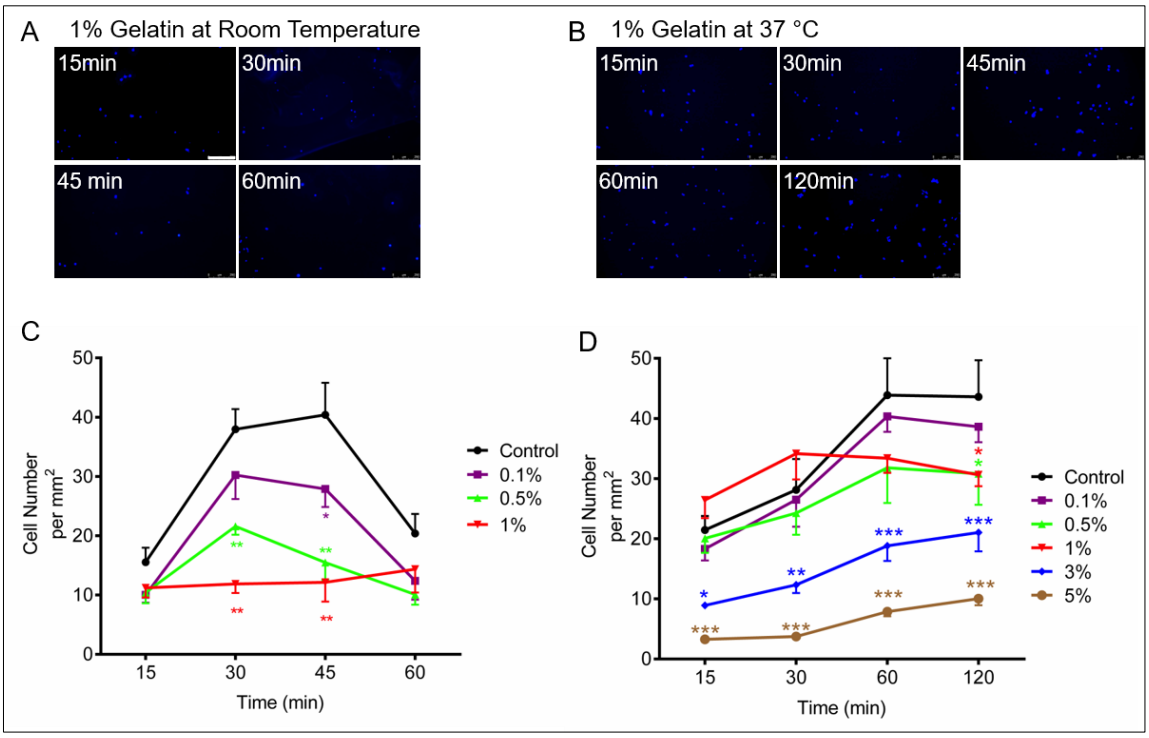

Figure 2 Gelatin delays attachment of RAECs to cell culture surface.
A. DAPI staining of cells in 1% gelatin attached to the bottom of a cell culture plate at room temperature over 1 hour. B. DAPI staining of cells in 1% gelatin attached to the bottom of a cell culture plate at 37 °C over 2 hours. C. Quantification of cell attachment over time for each gelatin concentration at room temperature. D. Quantification of cell attachment over time for each gelatin concentration at 37°C. *p<0.05, **p<0.01, ***p<0.001, vs. Control. Scale bar: 250 µm.

When the plates were cultured at 37°C, cell attachment was delayed in higher concentrations (3% and 5%) of gelatin (Figure 2D). Cell attachment tended to increase from 30 to 120 minutes in 3% and 5% gelatin mixtures, whereas the number of cells attached remained consistent from 60 to 120 minutes in all other groups, including the control group, indicating that all cells in the wells were already attached to the culture plate surface. On the basis of these results, we selected 1% and 5% gelatin concentrations for use in all in-vitro experiments.

2.4.3. Rat Aortic Endothelial Cell Survival, Proliferation, and von Willebrand Factor Expression Were Retained in the Presence of 1% Gelatin

To determine a concentration of gelatin that promoted cell attachment to the dECM without altering cell proliferation and survival, RAECs were cultured in the presence of 1% and 5% gelatin in medium for 7 days, after which cell viability, cell proliferation, and von Willebrand expression (vWF) were evaluated. A gelatin concentration of 1% did not alter cell viability; however, 5% gelatin decreased RAEC survival by 29.9% ($p<0.05$, Figure 3A). Cell proliferation significantly decreased in 5% gelatin ($p<0.05$, Figure 3B) but was not significantly affected in 1% gelatin. Finally, vWF expression on RAECs was not altered upon visual inspection in 1% gelatin but was qualitatively decreased in 5% gelatin (Figure 3C). Because these data showed lower cell viability, cell proliferation, and vWF expression in 5% gelatin, we chose to use 1% gelatin in all ex-vivo studies to increase cell attachment to ECM.

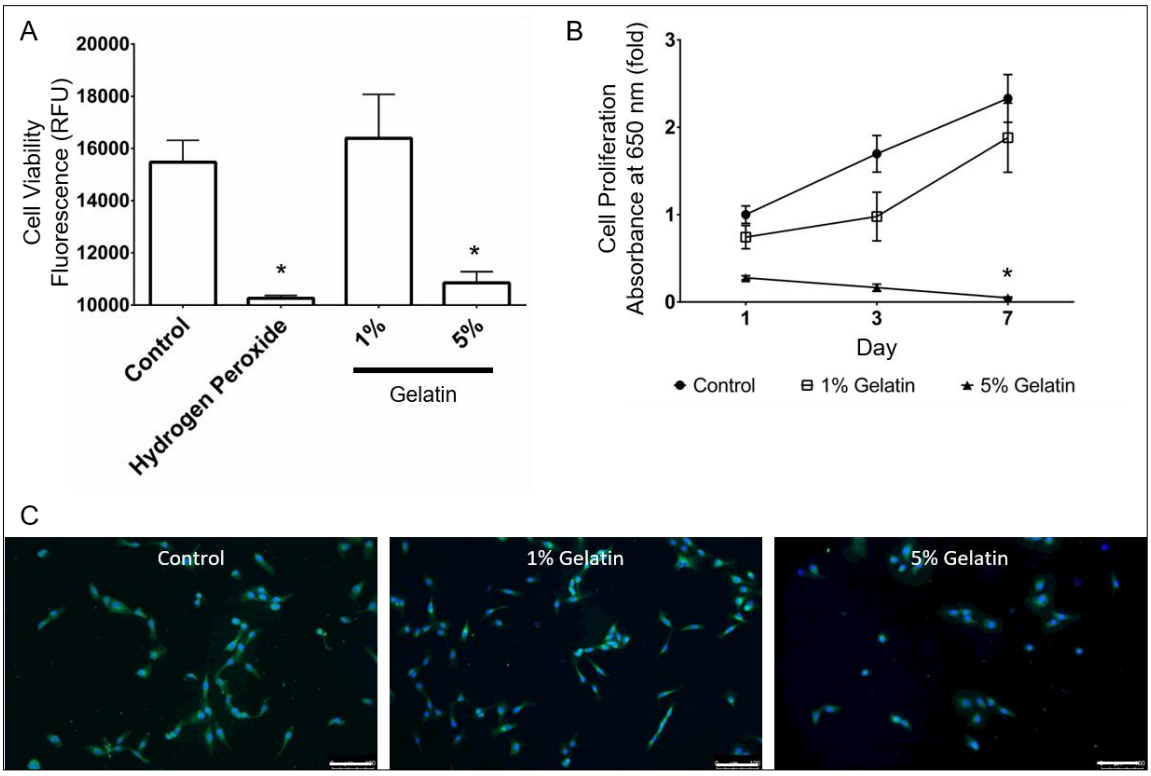

Figure 3 RAECs survive, proliferate, and retain von Willebrand Factor expression in 1% gelatin.
A. RAEC viability as measured by fluorescence using a cell viability assay kit. B. RAEC proliferation as measured by MTT assay up to 7 days. C. Immunofluorescent staining of von Willebrand Factor (vWF, green) associated with DAPI staining of nuclei (blue) confirms expression of vWF on RAECs in control (regular medium), 1% gelatin, and 5% gelatin. *$p<0.05$ vs. Control. Scale bar: 100 µm.

2.4.4. Gelatin Increased Endothelial Cell Retention in Rat Heart dECM

To test whether gelatin improved the cell retention of a re-endothelialized whole organ, cells were delivered to the cardiac vascular tree suspended in a media solution with and without 1% gelatin. RAECs (42 ± 3 million) were perfused into the coronary arteries of a rat whole heart dECM scaffold at a flow rate of 1 ml/min. The immediate retention of RAECs in both groups was higher than what was previously reported in published

studies.[13,30] Cell retention was significantly increased in the gelatin group (86 ± 2%, n=9) compared with the control group (58 ± 0%, n=14; $p<0.0001$; Figure 4A).

We measured the viscosity of media perfusate samples collected from the hearts daily for the first 5 days after re-endothelialization. A slight increase in the viscosity of the perfusate from the 1% gelatin group was observed only in the first day after RAEC perfusion. On the other days, the viscosity of the perfusate in the control and the 1% gelatin group was not significantly different and remained at an average of 0.90 mPa·s (Figure 4B), indicating that gelatin was no longer present in the solution.

At 7 days after endothelial cell infusion, we observed viable RAECs (CMFDA, green) with nuclear staining (Hoechst, blue) throughout the coronary vascular tree (Figure 5A). In hearts that were not recellularized with NRCMs, RAECs ware detected with DAPI staining throughout the vascular tree (Figure 5B).

2.4.5. Gelatin Promoted Retention of Cardiomyocytes in the Parenchyma of the Re-endothelialized Heart

To determine whether gelatin would increase cardiomyocyte retention in the cardiac parenchyma, we injected NRCMs (72 ± 6 million) in medium with and without 1% gelatin into the left ventricular free wall of re-endothelialized rat hearts 7 days after RAECs were perfused into the coronary vasculature without gelatin. After a period of 30 minutes without perfusion, more NRCMs were retained in the dECM when gelatin was present than when NRCMs were injected in medium alone (Table 3).

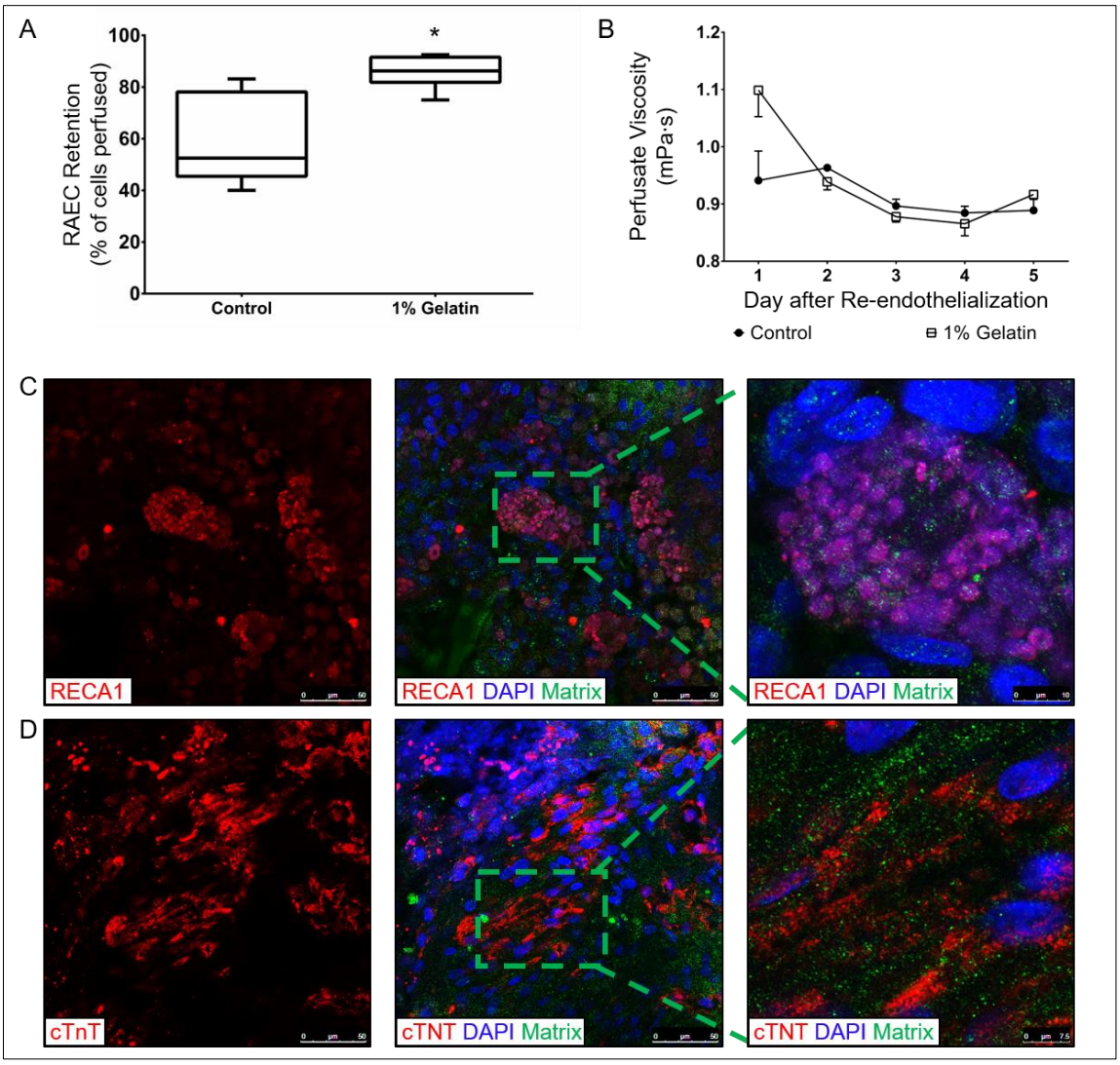

Figure 4 Endothelial cells and cardiomyocytes attach to decellularized cardiac matrix when delivered with gelatin.

A. One hour after RAECs were infused, the number of cells that flowed out of the heart was counted, and the percentage of retained cells was calculated. Gelatin increased the number of cells retained in the cardiac dECM vasculature 1 hour after infusion. B. Media perfusate samples collected from the heart on days following re-endothelialization show that immediately after re-endothelialization, the perfusate viscosity is increased when gelatin is present. After the first 48 hours, the perfusate viscosity is not different between the 1% gelatin and control media groups. C. Immunofluorescent staining showing rat endothelial cell antigen (RECA1)-positive cells clustered within matrix vessels. Surrounding cells in the matrix parenchyma do not exhibit positive RECA1 staining. D. Cardiomyocytes expressing cardiac troponin T antibody are within the matrix parenchyma of hearts recellularized with gelatin. *$p<0.0001$ vs Control.

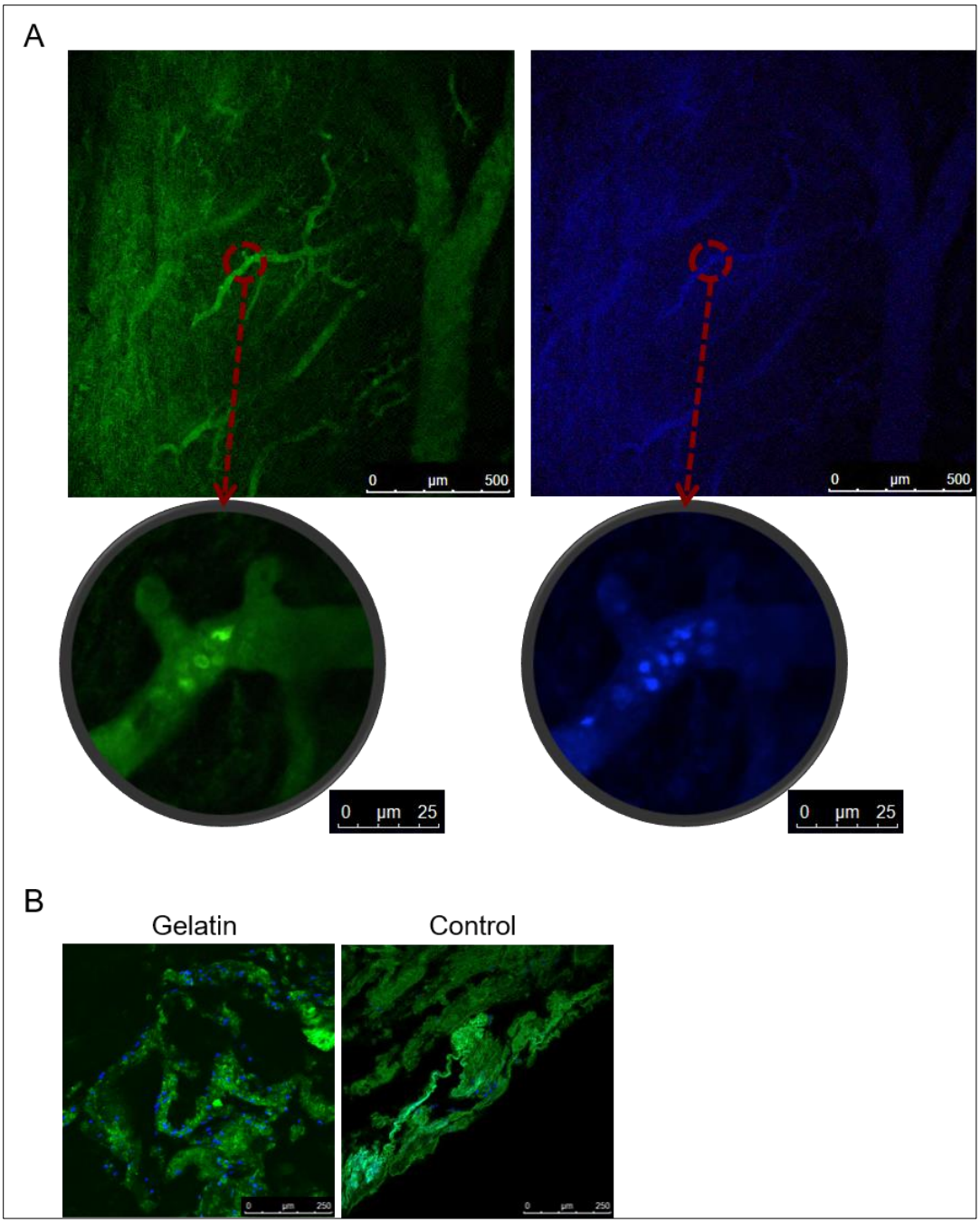

Figure 5 RAEC distribution in the vascular tree of decellularized rat heart.
A. Live CMFDA (green) and Hoechst (blue) staining of RAECs in whole heart 7 days after gelatin re-endothelialization showing cells within preserved vessel conduits of the re-endothelialized decellularized heart. B. Images of paraffin-embedded sections showing nuclei (DAPI, blue) and matrix (autofluorescence, green) in dECM after 7 days post-re-endothelialization with gelatin and in control without gelatin.

Table 3 Rat hearts recellularized with neonatal rat cardiomyocytes.

Recellularized hearts*	Total number of hearts injected	NRCMs retained after 30 minutes (%)	Recellularized beating hearts N (%)
Control	8	74.1 ± 3.2	1 (12.5)
1% gelatin	6	85.0 ± 1.8**	5 (83.3)

*Hearts were recellularized with neonatal rat cardiomyocytes (NRCMs) injected in medium only (Control) or in medium with 1% gelatin.
**P<0.05, versus Control.

Hearts were maintained for up to 35 days to observe contractility. Contractility was observed in 5 of the 6 hearts (83%) that were re-endothelialized and subsequently recellularized with NRCMs delivered in 1% gelatin, but in only 1 of the 8 hearts (13%) from the control group with RAECs and NRCMs delivered without gelatin (Table 3). Visible contractions started at day 5 in both groups and were maintained up to 35 days when hearts were harvested. Endothelial cells lined the vessels, whereas the cardiomyocytes were found in the parenchyma (Figure 4C and D, respectively). Integrin β1 expression was observed between cells and matrix in recellularized hearts (Figure 6).

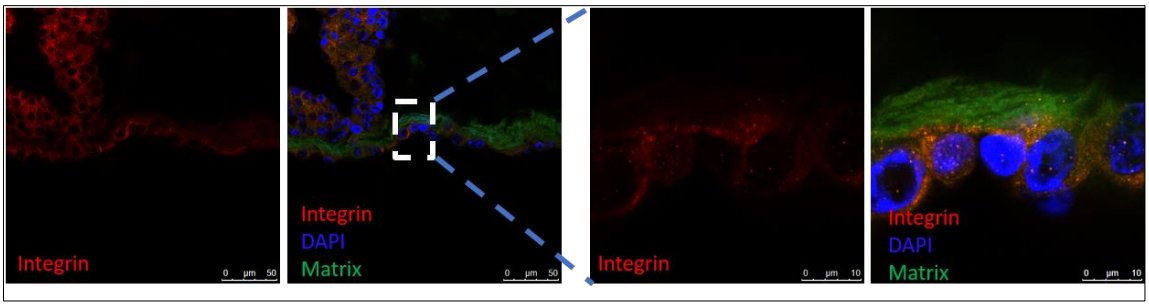

Figure 6 Expression of integrin on the membranes of RAECs in rat hearts re-endothelialized with gelatin.
Immunofluorescent staining of integrin β1 shows integrin expression on NRCMs in rat hearts recellularized with 1% gelatin.

2.5. Gelatin Aided in Pacing Cells in Desired Locations Throughout the Heart During Recellularization

After re-endothelialized and recellularized hearts were fixed and stained with Masson's trichrome staining, we examined cell distribution throughout the base, middle, and apex regions of the hearts. Qualitative comparisons of images taken from comparable regions of hearts showed differences in cell distribution in the base and apex. In control hearts, few cells were found in the basal region, but groups of cells were found in the apex (Figure 7A). However, in hearts recellularized with 1% gelatin, cells appeared more evenly distributed throughout the base, middle, and apex areas of the hearts (Figure 7B).

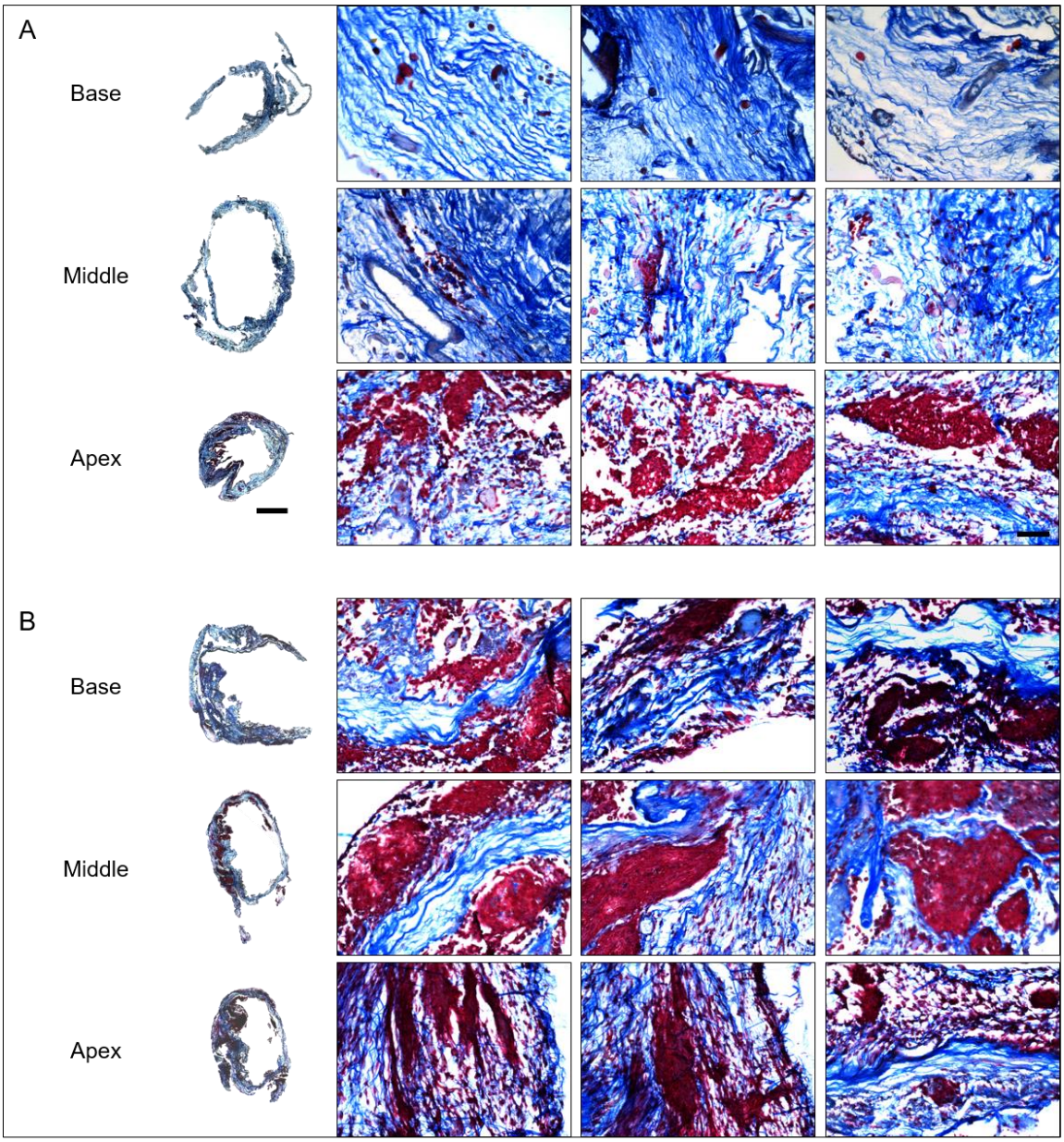

Figure 7 Cardiomyocytes distribution within the recellularized whole heart.
Trichrome staining of rat hearts re-endothelialized and recellularized with NRCMs with control medium (A) and 1% gelatin (B). A. Cell distribution is concentrated in the apex of the heart recellularized with control medium. Few cells are observed in the base of the heart. B. Cells are observed throughout the base, middle, and apex regions of the heart recellularized with 1% gelatin. Scale bar: 200 μm for cross-section images and 100 μm for close-up images.

2.6. Discussion

This study showed that delivering cells in gelatin–a biocompatible, viscous material–improves cell retention in a thick, vascularized, whole organ scaffold to generate a contracting heart. We demonstrated that gelatin promoted cell adhesion on the surface of a decellularized aorta, increased retention of RAECs delivered through decellularized vessel conduits into whole heart dECM, and improved NRCM contractility in rat heart dECM scaffolds. Using our improved cell delivery method with the addition of gelatin, we report the highest cell retention values in cardiac dECM published so far.[13,30,83] In our in vitro experiments, the increased gelatin-associated RAEC attachment in decellularized aorta was blocked by using a specific antibody against α5β1, indicating that integrin likely contributed to the improved cell attachment and retention observed in the dECM scaffold.

Gelatin is an ideal carrier for a wide range of applications, from a stabilizer in food products to a gelling agent in medical operations.[84] Gelatin is naturally derived from collagen and thus is biocompatible and biodegradable, making it ideal for use in biomedical systems.[85] Many groups have used gelatin in hydrogels cross-linked with other materials, such as glyceraldehyde[86] and chitosan,[87] to provide additional control over material properties[88,89]; however, this cross-linking can introduce toxic effects, reducing biocompatibility of the resulting hydrogel.[90,91] In our short-term in vitro experiments, we confirmed the biocompatibility of gelatin with endothelial cells, but 5% gelatin decreased viability and proliferation of endothelial cells over multi-day culture, a finding that has not been previously reported. Instead of cross-linking the 5% gelatin solution, we found that a lower 1% concentration of gelatin resulted in similar viability and proliferation of

endothelial cells as using media alone. As a result of our in vitro findings, we used 1% gelatin in further ex-vivo experiments. Our results indicate that gelatin can be used as a biocompatible carrier without any cross-linking but needs to be used within a proper working range to ensure long-term cell viability.

One of the main advantages of gelatin is that it can be used as an injectable carrier to target cell, drug, and growth factor delivery to a specific location.[92] Gelatin allows for the controlled release of drugs and growth factors,[93] but the delivery method can substantially affect how the final component acts at the delivery site.[94] Injected microspheres can have a controlled release,[95] whereas injected gelatin reduces cell scatter but degrades quickly.[91,96] For our study, we intentionally used unique delivery methods for each cell type so that infused endothelial cells would perfuse through the coronary vasculature and injected cardiomyocytes would be localized to cardiac parenchyma. As a result, we found cells in their specific cardiac compartments, with endothelial cells lining vessels and cardiomyocytes clustered in the left ventricular wall. Other investigators have used infusion and injection methods for recellularization of the whole decellularized heart,[16,28,43] but none has reported the addition of gelatin to the cell solution.

Another advantage of gelatin is its viscosity, which we controlled by manipulating the temperature and concentration of gelatin in solution. Initially, we tested high and low concentrations of gelatin to ensure suitable cell attachment, viability, and proliferation. We found that the lower concentration (1%) of gelatin fit our design criteria for increasing cell attachment to the matrix while not decreasing cell viability and proliferation. By lowering the temperature to room temperature (20°C) when 1% gelatin was first perfused

and injected into the dECM, we found that gelatin stayed in the local area. After giving the cells an opportunity to attach, we increased the temperature (37°C). At this higher temperature, the viscosity of the gelatin solution was the same as that in the media; therefore, the gelatin washed out, and the cells were able to interact with the natural environment of the dECM (Figure 4 and Figure 6). Having control over our tissue engineering methods is advantageous in that we can manipulate the process to retain more cells in the relevant compartments of the cardiac dECM bioscaffold and subsequently remove the cell carrier, which allows for the biologically driven remodeling of the ECM.[97]

Gelatin has been used as a scaffold or cell-sheet carrier in ocular,[98,99] osteogenic,[100] and chondrogenic[101] tissue engineering, but tissue engineering of a whole heart is challenging because of the need for a scaffold that has the mechanical and biological properties necessary to sustain beating over a patient's lifetime. The essential function of the heart is to contract and pump blood to the body, so having a dECM bioscaffold with the biomechanical and biochemical properties of elasticity[102] and preserved glycosaminoglycans[103] provides more mechanical and chemical cues so that cells function as in native tissue.[104] ECM derived from whole organs has the physical microstructure of the original organ, giving tissue-specific spatial cues to cells for organization.[105] Using gelatin as a cell carrier in cardiovascular tissue engineering helped to target cells to a specific location, but this was just the first step. Delivering cardiomyocytes to the parenchyma with gelatin helped to maintain contractile cells within the bioscaffold, which is an even more important endpoint.[106] We achieved a higher percentage of beating hearts with gelatin in the delivery solution than with media only, indicating that gelatin improves

not only cell retention but also cell function, which will aid in creating a fully functioning bioartificial heart. The relationship between cell retention and contractility is most likely closely linked as having more cardiomyocytes in the scaffold provides a greater overall contraction force.[107]

Although the mechanisms by which gelatin improves cell retention, and thus contractility, have not been identified, several factors may be at play. Gelatin could improve cell retention during recellularization via physical properties, cell morphological changes, mechanoreceptors, or a combination of these factors.

The physical properties of gelatin directly affect its ability to retain cells in a specific area. Gelatin offers tunable mechanical properties for delivering NRCMs into a specific region of interest. Increasing gelatin concentration in a solution increases the solution's viscosity,[108] as does decreasing the temperature.[109] In our study, when cells were infused at room temperature, adding 1% gelatin increased the viscosity of the cell suspension and increased cell retention by 28%, with cell retention rates higher than previously reported (10% to 54%).[13,30] Increasing solution viscosity with gelatin decreased the fluid loss during cell injection, resulting in increased cell retention. This increased viscosity could also increase friction between the plasma membrane of the cell and the ECM surface, causing cells to roll rather than slide along the vessel wall.[110] This rolling of the cells increases the surface area of the cell membrane that is exposed to the dECM, providing more opportunity for adherence and potentially contributing to increased endothelial cell retention in the recellularized matrix vessels. The ability to modify the physical properties of gelatin by adjusting the temperature provides significant advantages

in this approach. The viscosity of gelatin at room temperature improves cell retention, and increasing the temperature leads to the removal of gelatin from the matrix. This manipulation of temperature allows important cell-matrix interactions to occur by maximizing spatiotemporal cell-ECM exposure.[111]

Another mechanism for improving cell attachment with gelatin may relate to morphological changes in the cells. The higher solution viscosity caused by the addition of gelatin can increase shear stress, which can promote cell retention and attachment to dECM by changing cell shape. Shear stress is the product of viscosity times the shear rate, which is determined by the diameter of the vessel, as per Newton's Law. Given this, with a constant vessel diameter, shear stress increases when viscosity is increased. Thus, when cells are suspended in a gelatin solution, the shear stress and cell deformation increase within a fixed-diameter vessel.[112] Furthermore, cell shape and morphology are critical predictors of endothelial cell spreading.[113-115] When cells enter the flow stream in the coronary vasculature, their shape is determined by the shear stress.[116,117] Therefore, this increase in shear stress combined with the viscosity of the gelatin may lead to increased spreading and attachment of endothelial cells to the dECM.

Lastly, another possible contributing factor is an alteration in the mechanosignaling at the cell surface, which can mediate cell adhesion and attachment. Shear stress can activate adhesion molecules and receptors on the endothelial cell membrane, causing downstream signaling of molecules such as receptor tyrosine kinases, integrins, G protein-coupled receptors, and stretch-activated ion channels.[118-120] Many of these mechanoreceptors mediate cell attachment. As shear stress increased during

perfusion in the vasculature with gelatin, the affinity of cells for the matrix may have also increased due to shear stress-induced activation of adhesion molecules. In addition, NRCM adhesion to matrices may be mediated by integrin receptors acting as mechanoreceptors.[121,122]

Together, our results build on existing applications of gelatin and suggest that gelatin, when used as a cell delivery vehicle, can improve recellularization in cardiac tissue engineering studies. Additional work is warranted to identify specific factors involved in the interactions between cells in gelatin and the dECM. We conclude that the presence of viscous gelatin promotes cell attachment and retention within the dECM vasculature and parenchyma.

2.7. Conclusion

Gelatin should be considered as a potential biocompatible cell carrier to increase cell retention during recellularization of dECM and to support re-endothelialization of the whole heart.

2.8. Supplementary Methods

2.8.1. RAEC Attachment to Tissue Culture Plate in Increasing Concentrations of Gelatin

RAECs were resuspended in 0.1%, 0.5%, 1%, 3%, 5% gelatin, or control medium without gelatin. Cells in suspension were plated in 96-well plates at a density of 5000 cells/cm^2. Plates were kept at room temperature for 60 minutes or in a 37°C incubator for 24 hours. At 15-minute, 30-minute, 45-minute, and 1, 2, 4, and 24-hour time points, cells attached to the bottom of the well were washed and fixed in 2% paraformaldehyde before being

stained with DAPI. The number of nuclei per 1.35 mm^2 was counted manually. For the samples at room temperature, only cells in 1% gelatin or less were counted due to the gelation of samples at higher concentrations after 15 minutes.

2.8.2. Live Cell Immunofluorescence Staining in the Whole-mount Heart Tissues

To detect viable cells in the vasculature of the whole heart at day 7 after cell infusion, we visualized metabolically active cells after incorporation of CellTracker CMFDA Green (10 µM, Thermo Fisher Scientific, USA). Simultaneously, dead cells were labeled with propidium iodide (500 nM, Sigma-Aldrich, USA), and nuclear material was stained with Hoechst 33342 dye (100 µg/ml, ThermoFisher Scientific, USA). Cells were incubated with dyes for 30 minutes in the perfusion system at 37ºC. Fluorescent images of the stained recellularized whole-mount heart samples were obtained using a Leica SP5 confocal microscope (Leica, Germany).

3. DECELLULARIZED CARDIAC EXTRACELLULAR MATRIX INCREASES CARDIOMYOCYTE ELONGATION AND CONTRACTILITY IN TISSUE ENGINEERED CARDIAC RINGS

3.1. Synopsis

3.1.1. Introduction

Cardiomyocyte elongation has been linked to enhanced myofilament organization, which contributes to overall cell contractility and functionality. While tissue scaffolds have been engineered to induce cell elongation using topographical cues, decellularized cardiac extracellular matrix (dECM) bioscaffolds are known to be bioactive and retain native cues for cell organization and regeneration, including the alignment of stem cells. However, the effects of the native extracellular matrix on cardiomyocyte elongation and contractility are still unknown.

3.1.2. Hypothesis

We hypothesized that dECM increases elongation and contractility of neonatal rat ventricular cardiomyocytes (NRVCMs) versus engineered collagen constructs, resulting in physiologically-relevant, scalable tissues for cardiovascular tissue engineering.

3.1.3. Methods and Results

Adult rat hearts were harvested and perfusion-decellularized through the coronary vasculature under constant pressure. Hearts were sectioned on a vibratome transversally to create 300 μm-thick rings of the left ventricle. Collagen (type 1) rings of the same size as the dECM rings were made by using rat tail collagen (2.0 mg/ml). Ten million

NRVCMs were isolated, purified, and injected into the left ventricle of dECM or collagen rings (n=12 each). Cell survival, distribution, elongation, and alignment were evaluated after 14 days by using immunofluorescence and confocal microscopy. The dECM significantly increased nuclear elongation (major to minor axis ratio of 1.585 for cells in dECM vs. 1.37 in collagen, n=6 each, $p<0.01$). Microscopic contractions were observed in dECM as early as day 3 (n=3). The number of spontaneous contractions of cells in dECM (n=5) was significantly greater than that in collagen (n=3) ($p<0.01$), as observed by atomic force microscopy.

3.1.4. Conclusion

In conclusion, dECM increased cellular elongation and contraction frequency of neonatal rat ventricular cardiomyocytes, suggesting the presence of tissue-specific cues in the extracellular environment of cardiomyocytes is beneficial for tissue function. Studies utilizing human stem-cell derived cardiomyocytes are underway to verify the organizational, functional, and physiologic properties of recellularized dECM.

3.2. Introduction

With the rise of cardiovascular disease in the world, more therapies are needed that will replace or restore the diseased heart. In tissue engineering, scientists and engineers aim to create native-like tissue by using cells, bioactive signals, and scaffolds for organ repair and regeneration, in addition to potential drug testing and disease modeling. Unique to cardiovascular tissue engineering is the need to create contracting tissue constructs that match or augment the contractile performance of native cardiac tissue. A major component of cardiac tissue contractility is cellular organization.[123] During development,

cardiomyocytes are grouped into myocyte bundles and organized into myolaminae. The complex and intricate extracellular matrix (ECM) that surrounds cardiomyocytes and other cardiac cells provides structural organization so that upon contraction, cells can transmit force that results in a full organ heartbeat.[124-126]

Enhanced myofilament organization contributes to overall cell contractility and functionality and is known to be linked with cardiomyocyte elongation. In native development, cardiomyocytes gradually elongate and align themselves into fiber tracts.[127] Bioengineers use external forces to direct cellular organization *in vitro*. Methods to drive cellular organization and elongation include: encapsulation,[128] micropatterning,[129] and nanotopography.[130] These human-made tissue scaffolds induce cell elongation using topographical cues, which drive cells to increase contractility due to a given shape. A disadvantage of such direction is the stress put on the cells during maturation. Since we first perfusion-decellularized the whole heart, our lab has pioneered the use of decellularized extracellular matrix (ECM) as a naturally-derived bioscaffold for cardiovascular tissue engineering.[13]

Decellularized ECM (dECM) bioscaffolds are advantageous because they retain the complex and intricate architecture of native ECM. Perfusion decellularization preserves the native biochemical and mechanical cues for cell organization and regeneration, including the alignment of stem cells.[131] However, the effects of the decellularized cardiac extracellular matrix on cardiomyocyte elongation and contractility are still unknown.

Stem cells in the dECM are contact-guided into alignment with ECM matrix fibers, but it is unknown if cardiomyocytes respond in the same way by organizing and subsequently contracting. The present study aimed to create human pediatric-sized cardiac rings with recellularization above the previously reported 33.8% viability in a recellularized tissue[13], with elongated cellular structure and with measurable cardiac tissue contractions. We report the creation and characterization of cardiac rings made from hiPSC-CMs in rabbit cardiac dECM bioscaffolds.

3.3. Materials and Methods

3.3.1. Rat Heart Harvest and Decellularization

All experiments were performed in accordance with the US Animal Welfare Act and were approved by the Institutional Animal Care and Use Committee at the Texas Heart Institute. Fischer 344 rats (Charles River, Wilmington, MA) were anesthetized with 5% isoflurane and then heparinized with 1000 UI/ml sodium heparin intraperitoneally. The thoracic cavity was opened through a median sternotomy to expose the heart and its branching vessels. The brachiocephalic artery was ligated and cut. The aorta, superior vena cava, inferior vena cava, left pulmonary artery, and pulmonary veins were cut to remove the heart. The aorta was cannulated with a 1 mm cannula, and the heart was flushed with PBS. Decellularization was modified from the previously described protocol. Hypertonic, hypotonic, and 1% SDS solutions were perfused sequentially through an aortic cannula at a constant pressure of 70 mmHg for 10, 10, and 30 hours, respectively. Lastly, PBS was perfused at a flow rate of 5 ml/min for 24 hours. The decellularized hearts were stored in PBS at 4 °C for recellularization at a later timepoint. Before re-

endothelialization, hearts were incubated with penicillin (100 U/mL) and streptomycin (100 µg/mL), and amphotericin B (2.5 µg/mL, Sigma-Aldrich, MO) in PBS at 37°C for at least 8 hours and stabilized with medium at 37°C for at least 8 hours.

3.3.2. Isolation and Preparation of Neonatal Rat Cardiomyocytes

Neonatal Sprague Dawley rats (1-3 days old) (Texas Animal Specialties, TX) were euthanized with an intraperitoneal injection of sodium pentobarbital 100 mg/kg and heparin 150 mg/kg. Hearts were excised and immediately placed into PBS on ice. Hearts were minced and placed into Hank's Balanced Salt Solution (HBSS) with Trypsin (10,000 U/mL, (Sigma-Aldrich, MO) at 4 °C overnight. Hearts were digested in a solution of collagenase type II 200 U/mL (Worthington Biochemical Co., NJ) and 0.06% pancreatin (wt/wt, Sigma-Aldrich, MO) solution at 37 °C. The digested cells were collected and passed through a 100 µm cell strainer. Cells were placed in T-175 flasks and incubated for 1 hour to allow fibroblasts to attach to the flask. The supernatant was collected and plated for another hour to further reduce the number of fibroblasts. The final supernatant, enriched for greater than 95% cardiomyocytes[132], was collected and used for neonatal rat ventricular cardiomyocyte (NRCM) injection into the decellularized heart.

3.3.3. Creation of Collagen and Rat dECM Cardiac Rings

Collagen (type 1) rings were made by using rat tail collagen (2.0 mg/ml). The diameter of the synthetic gel ring was approximately 11.6 mm. The collagen was kept on ice and mixed with the cell media before being titrated with sodium hydroxide to a pH of 7.4. The collagen liquid mixture was then pipetted into a rubber mold that held the collagen during gelation for 2 hours in a 37°C, 5% CO_2 incubator.

Perfusion-decellularized rat hearts were sectioned on a vibratome transversally to create 300 µm-thick rings of the left ventricle. Ten million NRCMs were injected into rings using a syringe pump with a flow rate set at 5 µl/min. For dECM rings, a total of 3 injections of 5 µl each were made in the left ventricle free wall and 1 injection of 5 µl into the septum. The collagen rings had no right ventricle, so the four injections were equally spaced around the ring. A total of 20 µl was injected into each ring (Figure 8).

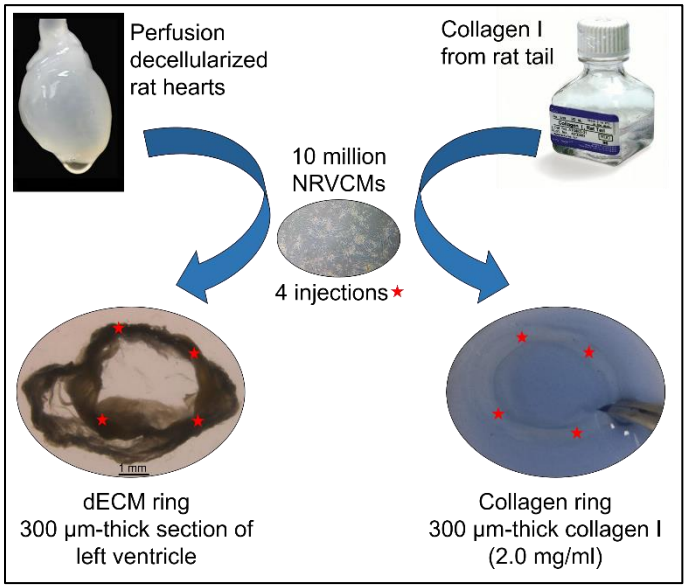

Figure 8 Methodology of creating rat cardiac ring and collagen ring.

3.3.4. Contractility

Rings were observed every day for spontaneous contractions. Video of contractions were recorded using a light microscope with 10x objective lens. Cardiac rings remained in the tissue culture plate wells in which they were cultured; rat cardiac dECM

rings were cultured in 48-well plates, and rat collagen rings were cultured in 24-well plates. Tissue culture plates were placed on the microscope stage for video recordings. All recordings were collected with a Leica DMI3000B microscope. Optical analysis was performed using a video analysis and model tool (Tracker,[133] Version 5.0.6; Open Source Physics, 2018) to determine the contraction displacement and frequency using pixel-tracking.

3.3.5. Nuclear Elongation

After 14 days in culture, collagen and rat cardiac rings were rinsed with PBS and fixed in 4% paraformaldehyde at 4 °C overnight. Rabbit cardiac rings were cultured for 7 days before sample fixation. Samples were stained with DAPI (4',6-diamidino-2-phenylindole) and laminin γ1 (ab11575, Abcam, MA). Images were taken using a Leica SP5 confocal microscope. Images were processed in ImageJ to outline the nuclei, measure the major and minor axes, and determine the nuclear angle.

3.3.6. Statistical Analysis

The continuous variable nuclear elongation was expressed as mean ± SEM. Student's t-test was used for two group comparisons. A p-value less than 0.05 was defined as significant. All data for statistical analysis were processed with Graph Pad Prism 5.0 (Graph Pad Software Inc., CA).

3.4. Results

3.4.1. NRCMs Survive and Attach in Collagen Cardiac Rings and Rat dECM Cardiac Rings

When NRCMs were injected into collagen and rat dECM cardiac rings, the cells survived for 14 days in culture, at which point the cardiac rings were fixed with paraformaldehyde and processed for further evaluation. Following immunofluorescent staining for matrix protein laminin γ1 and DAPI, the distribution of cells was observed in their respective ECM environments (Figure 9). Cells were distributed throughout the rat dECM cardiac ring. Likewise, NRCMs were observed throughout the collagen rings.

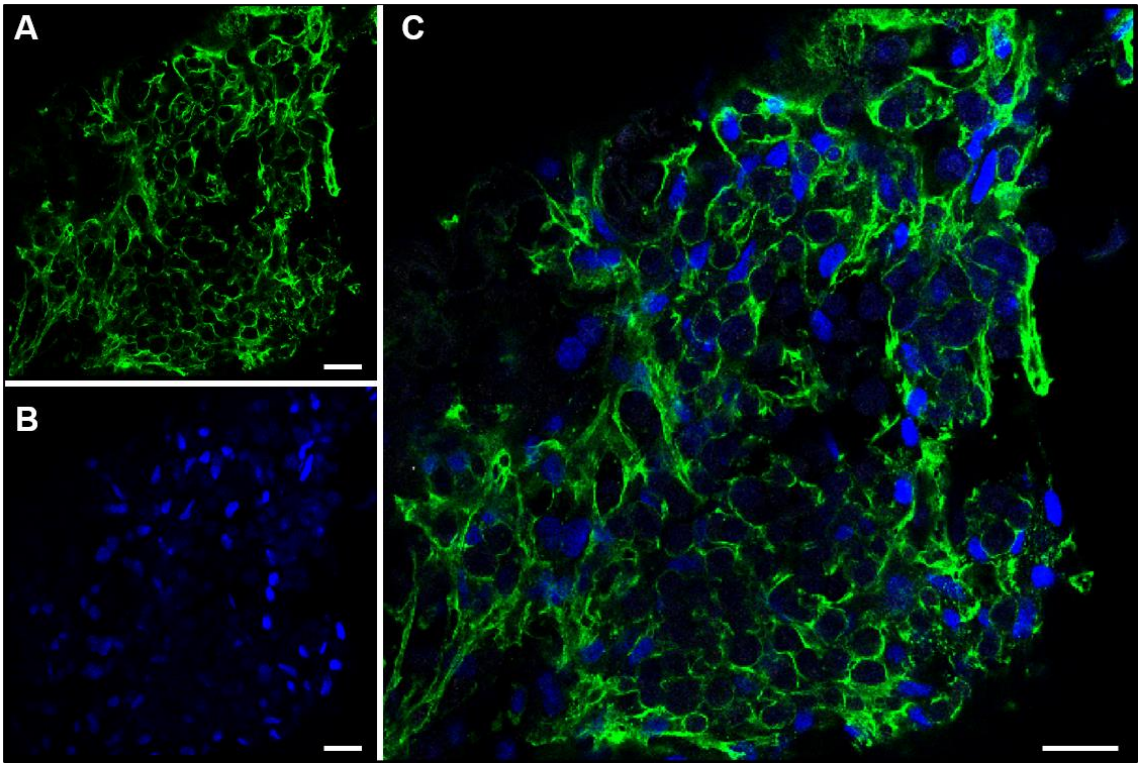

Figure 9 NRCM survival and attachment in decellularized ECM rings.
Cells attached to the ECM throughout the ring after 14 days. Cell distribution within the matrix was observed by staining for: (A) laminin and (B) nuclei. (C) Merged images of stained laminin (green) and nuclei (blue). Scale bar: 25 µm.

3.4.2. Cells Elongate in dECM

Images of matrix protein and DAPI staining were recorded for cells in rat collagen, rat dECM, and rabbit dECM. The major and minor axes of each nucleus was measured using ImageJ software analysis. The elongation of each nucleus was calculated by using the ratio of the major to minor axis. The average elongation of NRCMs was 1.379 ± 0.323 in rat collagen (n = 263 nuclei) and 1.585 ± 0.494 in rat dECM (n = 243). Overall, cells in dECM were significantly more elongated than cells in collagen cardiac rings (Figure 10).

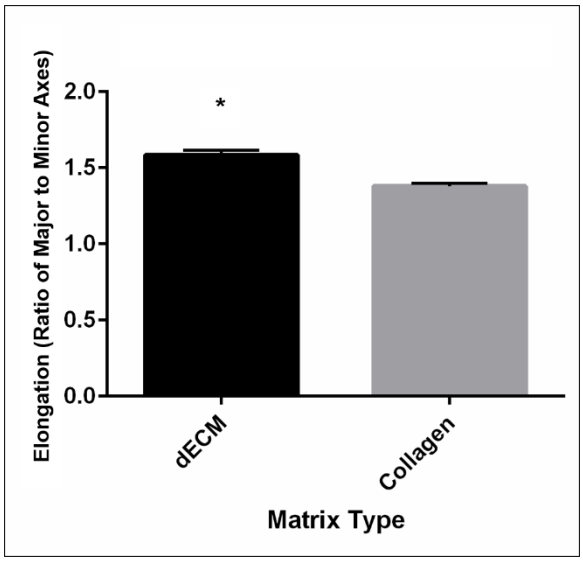

Figure 10 Nuclear elongation of cells in rat dECM cardiac rings and collagen rings. Cells were more elongated in the dECM cardiac ring than in the collagen ring. $p<0.00001$.

3.4.3. Cells in Collagen and dECM Spontaneously Contract

Spontaneous contractions were observed in cardiac rings of collagen, rat dECM, and rabbit dECM as early as day 3 after cell injection and continued until day 7. Movement of the rings was recorded at 10x magnification, and videos showed obvious tissue movement beyond single cell capability. In some areas, the rings contracted in a coordinated matter with the tissue moving as a whole unit (Figure 11). However, most contractions occurred in sporadically in independent locations around the left ventricular free wall.

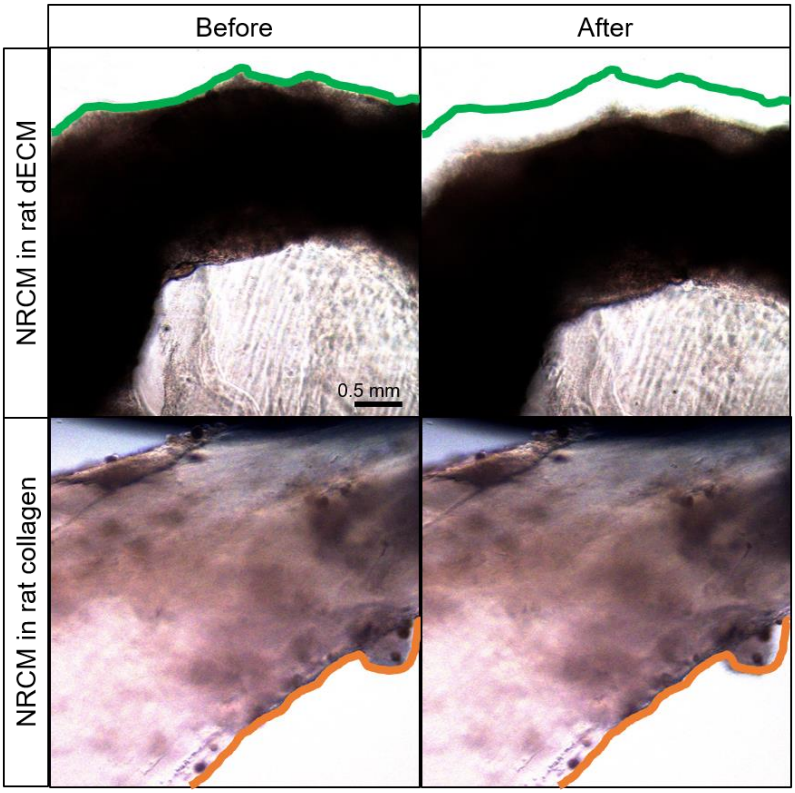

Figure 11 Spontaneous contractions of NRCMs in rat dECM cardiac rings and collagen rings.

3.5. Discussion

In this study, we report the creation of cardiac rings made by recellularized rat cardiac dECM bioscaffolds. We found that NRCMs in cardiac dECM had increased contraction and nuclear elongation when compared to NRCMs in collagen rings.

Bioengineers have long used synthetic- and biologically-derived materials for creating cardiac tissue constructs with the end goal of creating functional cardiac tissue. One factor in CM contractility is driving the cells to elongate and organize within scaffolds. Previous studies have used tools such as microcontact printing,[134] nanopattern

topography,[135,136] and electrospinning[137] to reorganize cells in scaffolds. However, in this study, we used a bioscaffold that has the native cardiac ultrastructure. Since decellularization preserves the native macro- and micro-architecture,[138] organization of CMs is directed by biochemical and biomechanical cues of the native cardiac ECM.

By comparing the native dECM bioscaffold with a biologic-derived collagen scaffold, we saw that NRCMs were more elongated in dECM than in collagen, suggesting that the native biological, biochemical, and structural cues of the native cardiac ECM were modulating CM elongation. The more the CM is elongated, the higher the contraction force.[135] The form of the CM directly affects the function of the CM,[139] with a less elongated cell shape unable to produce enough physical force for contraction.[140] By organizing cells into an elongated shape, the dECM provides the optimal shape for CMs to generate a contraction strong enough to make the cardiac ring beat.

Currently, we in the field of cardiac tissue engineering have not been able to create a cardiac tissue that fill the contractile needs of the beating heart. Thus, continuing to improve the organization of the cells through bioscaffold cues produces stronger cardiac tissues that can be further trained with other stimuli to replace damaged or fibrotic cardiac tissue in vivo.

Another improvement in the recellularization of decellularized left ventricular rings was the number of cells attached and distributed throughout the ring after 7 days in the rabbit dECM. The cellularity of the cardiac rings had an average of 63.3% when compared with native human cadaveric tissue. It is important to note that other labs do not report the cellularity in their recellularized or re-vascularized constructs, and most

percentages reported are cells retained in the whole organ.[13,30] By having a way to quantify the recellularization technique, we can see how the number of cells present in the construct directly affects its function. If we further increased the cellularity to be on par with the native human tissue, we may be able to obtain contractions that grow in strength as cells mature and become coupled with neighboring cells.

Future studies will focus on generation of stronger contractions in larger scaffold constructs, which may result from application of biophysical stimuli or chemical signals. Coordinated and more forceful contractions can be seen with mature electrophysiological structures in cardiomyocytes.[141] Many factors have been used to drive electrophysiologic maturation, including stretch, substrate stiffness, and electrical stimulation. Studies are ongoing in our lab to use both electrical and mechanical stimulation to increase the construct contractility to achieve more native-like tissue in vitro.

Moreover, not only will external stimuli improve cardiomyocyte contractility, but also development of larger recellularized scaffold constructs could potentially generate more force; however, a major hurdle in creating larger solid organs is the number of cells needed to recellularize the whole organ.[142] Billions of cells would be needed to generate the contraction force required to visualize contractions and to achieve the goal of generating a bioartificial heart using cardiac dECM.[143] Even so, scientific advancements, such as the creation of human induced pluripotent stem cells, make this goal attainable. Since cardiomyocytes have a low proliferative capacity, billions of patient-derived hiPSCs can be grown in vitro,[144] then differentiated into patient-specific hiPSC-derived cardiomyocytes for cardiovascular tissue engineering.[145] Future studies will incorporate

multiple biotechnologies of decellularization and hiPSC expansion to build a bioartificial heart.

4. ELECTROPHYSIOLOGICAL MATURATION OF CARDIAC RING-EMBEDDED HUMAN CARDIOMYOCYTES BY COMBINED ELECTROMECHANICAL STIMULATION IN A CUSTOM BIOREACTOR

4.1. Introduction

Tissue engineering aims to create native-like tissue by using cells, bioactive signals, and scaffolds for potential drug testing, disease modeling, and organ repair and regeneration.[9,10] To create bioengineered tissue constructs with clinical potential, scientists have identified induced pluripotent stem cells (iPSCs) as a potential cell source, since they can be generated from adult somatic cells, can be expanded several orders of magnitude *in vitro,* and can be differentiated into multiple cell lineages, including cardiomyocytes (CMs).[45] The use of human iPSC-derived CMs (hiPSC-CMs) allows scientists to develop and screen therapies for patient-specific genetic diseases *in vitro*[46] because hiPSC-CMs appear to retain disease phenotypes.[47,48] However, once differentiated into cardiomyocytes, hiPSC-CMs have a low proliferative capacity[49] and an immature cardiac phenotype.[50]

Analysis of the electrophysiological[51-53] and structural[54,55] characteristics of hiPSC-CMs reveal a phenotype that lies between early fetal and adult CMs. While hiPSC-CMs display key properties such as cardiac-type action potentials and an excitation-contraction coupling mechanism that confirm their CM identity, other properties, such as calcium handling, conduction velocity, and contractile properties, do not reflect those observed in adult CMs. Since hiPSC-CMs are phenotypically comparable to immature

CMs *in vivo*, some of the same factors that influence maturation in embryonic and fetal development may be used to promote hiPSC-CM maturation *in vitro*.[56] Enhancing hiPSC-CM maturation is critical to engineer physiologically accurate models of the adult heart, to perform disease-specific drug screens, and to repair damaged or diseased native myocardium.[57] By taking cues from nature, we hypothesized that by combining three key factors that promote hiPSC-CM maturation *in vivo* and *in vitro* – (1) extracellular matrix (ECM) cues, (2) electrical stimulation, and (3) mechanical loading – we would achieve electrophysiological and structural hiPSC-CM maturation beyond what is reported in the literature.[146]

Altogether, electrical field stimulation and mechanical stretch have been shown to improve hiPSC-CM electrophysiological and structural properties *in vitro*; however, few studies show their combined effects on CMs in synthetic scaffolds or hydrogels.[147-149] Additionally, these studies have not examined hiPSC-CMs in cardiac dECM. We hypothesized that combined mechanical and electrical stimulation synergistically increased electrophysiological and structural maturation above what is observed by electrical and mechanical stimulation alone. We aimed to fill this knowledge gap by measuring the effects of combined electrical and mechanical stimulation on cardiac rings made from cardiac dECM injected with hiPSC-CMs, in order to establish a biophysical stimulation paradigm for driving hiPSC-CM maturation in dECM.

4.2. Materials and Methods

4.2.1. Rabbit Heart Harvest and Decellularization

All experiments were performed in accordance with the US Animal Welfare Act and were approved by the Institutional Animal Care and Use Committee at the Texas Heart Institute. New Zealand white rabbits (Charles River, Wilmington, MA) were anesthetized and heparinized. Rabbits were euthanized under deep anesthesia, and a medial sternotomy was performed. The aorta, superior vena cava, inferior vena cava, left pulmonary artery, and pulmonary veins were cut to remove the heart. The aorta was cannulated, and the heart was flushed with PBS. Hypertonic solution (500 mM NaCl), hypotonic solution (20 mM NaCl), 1% SDS solution, 1% peracetic acid in 1% SDS solution were perfused sequentially through an aortic cannula at a constant pressure of 60 mmHg for 5, 5, and 50 hours, and 10 hours respectively. Lastly, PBS was perfused through the heart for 24 hours. The decellularized hearts were stored in PBS at 4 ° C.

4.2.2. Differentiation and Culture of hiPSC-CMs

Human iPSCs were obtained from the Stanford Cardiovascular Institute Biobank Lab and differentiated into CMs using the STEMdiff Cardiomyocyte Differentiation Kit per manufacturer's instructions (STEMCELL Technologies, MA, USA). Differentiation efficiency was quantified using flow cytometry using cardiac troponin as a positive marker for cardiomyocytes. Only cell batches with differentiation efficiencies of greater than 65% cardiac troponin-positive cells were used for recellularization.

4.2.3. Creation of Rabbit dECM Cardiac Rings

Perfusion-decellularized rabbit hearts were sectioned transversally using a rabbit heart mold to create 1 mm-thick rings of the left ventricle. One million hiPSC-CMs were injected into rings at 6 different locations around the left ventricle, including the septum (Figure 12).[150] The right ventricular wall was not injected with cells.

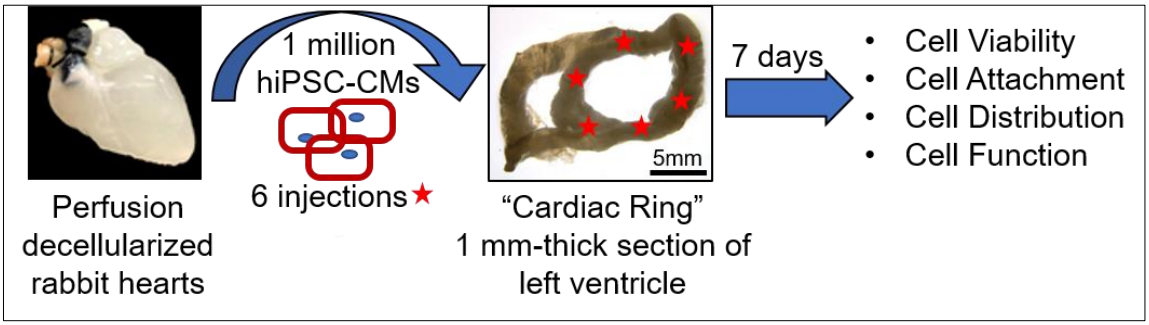

Figure 12 Method for creating rabbit dECM cardiac rings.

4.2.4. Cell Viability and Cellularity in Rabbit Cardiac Rings

After 7 days in culture, cell viability in rabbit cardiac rings was quantified by measuring NADH dehydrogenase activity in the culture media using Cell Counting Kit-8 following the manufacturer's instructions.[151]

After measuring cell viability, the cardiac rings were fixed in 2% paraformaldehyde in PBS at 4 °C overnight in preparation for immunofluorescence staining. A standard immunostaining procedure was carried out for matrix proteins collagen I, laminin and fibronectin and DAPI. Whole rings were stained using an anti-collagen I antibody (ab34710, Abcam, MA), anti-laminin γ1 antibody, and anti-fibronectin

antibody (ab2413, Abcam, MA). Fluorescently-labeled secondary goat anti-rabbit IgG, Alexa Fluor 488 conjugate antibody (ThermoFisher Scientific, CA) was used. Samples were then stained with DAPI. Six representative images around the recellularized left ventricular ring were recorded using a confocal microscope (Leica). The cell number and matrix area for each image was calculated using ImageJ image analysis. The cell number per matrix area was calculated for each image and extrapolated to yield an average ring cellularity relative to a sample from a human cadaveric heart.

4.2.5. Biophysical Stimulation

After 24 hours in support media after recellularization, cardiac rings were placed into a closed bioreactor for mechanical (M-Stim, 2.5% stretch, 1 Hz), electrical (E-Stim, 5 V, 2 ms duration, square waveform, 1 Hz), combined electromechanical stimulation (E/M-Stim, 5V, 2 ms duration, square waveform, 1 Hz, 2.5% stretch, 1 ms delay), or no stimulation (Non-Stim). After the cardiac rings were cultured in the bioreactor chambers for 7 days, the cardiac rings were removed from the bioreactor and evaluated for contractility, nuclear elongation, and electrical activity.

4.2.6. Multi-Electrode Array

Electrical activity from the cardiac rings were recorded using a MultiChannel Systems multi-electrode array (MEA). After being removed from the bioreactor main chamber, the cardiac rings were placed on a glass ecoMEA (MultiChannel Systems MCS GmbH, Germany) and kept warm using a temperature-controlled plate during recording. Electrical activity was recorded using 60 electrodes in a 5mm x 5mm grid. The cardiac rings were moved between recordings to measure multiple areas in one cardiac ring. Data

analysis of the electrical recordings was completed using MC Rack (MultiChannel Systems MCS GmbH, Germany) and LabChart (ADInstruments, Australia). The field potential duration (FPD) in milliseconds and beat frequency in Hertz were recorded and analyzed in multiple electrodes across the MEA using LabChartPro Software from ADInstruments (New Zealand).

After the baseline electrical signal was recorded, dobutamine was administered to one cardiac ring from each group was treated with a β_1-adernergic agonist and the response was recorded with the MEA. Dobutamine is used clinically to increase contractility and cardiac output[152], and we applied it to the cardiac rings during the MEA recordings in three increasing concentrations: low (5 μg/ml), medium (50 μg/ml), and high (500 μg/ml) doses.

4.2.7. Nuclear Elongation

After 7 days in culture, cardiac rings were prepared for immunostaining of matrix proteins and nuclei to assess nuclear elongation. Briefly, cardiac rings were rinsed with PBS and fixed in 4% paraformaldehyde at 4 °C overnight. Samples were stained with DAPI (4',6-diamidino-2-phenylindole) and with primary antibodies for matrix proteins collagen I (anti-collagen I antibody, ab34710, Abcam, MA), laminin γ1 (anti-laminin γ1, ab11575, Abcam, MA), and fibronectin (anti-fibronectin antibody, ab2413, Abcam, MA). Fluorescently-labeled secondary goat anti-rabbit IgG, Alexa Fluor 488 conjugate antibody (ThermoFisher Scientific, CA) was used. Images were taken using a Leica SP5 confocal microscope. Images were processed in ImageJ to outline the nuclei, measure the major and minor axes, and determine the nuclear angle.

4.2.8. Statistical Analysis

Continuous variables QT interval, beat frequency, and nuclear elongation were expressed as mean ± SEM. Outliers were detected and removed from data sets using the ROUT method by identifying outliers from a nonlinear regression with Q=0.01%.[153] One-way ANOVA test with multiple comparisons was used for four group comparisons. A p-value less than 0.05 was defined as significant. All data for statistical analysis were processed with Graph Pad Prism 8.0 (Graph Pad Software Inc., CA).

4.3. Results

4.3.1. hiPSC-CMs Survive and Attach in Rabbit dECM Cardiac Rings

One million hiPSC-CMs were injected in rabbit dECM rings to create recellularized cardiac rings. The cardiac rings were cultured for 7 days in hiPSC-CM maintenance media. Between days 3 and 7 after injection, cardiac rings were observed to spontaneously contract when viewed using the microscope under 10x objective lens. Contractions that were observed to start on day 3 continued until constructs were fixed for immunofluorescent staining on day 7.

Following immunofluorescent staining for matrix proteins laminin, fibronectin, and collagen I, the presence and location of cells within the matrix were observed. Whole mount tissues stained for integrin β1 showed positive staining between cells and matrix, confirming cell attachment to the matrix (Figure 13).

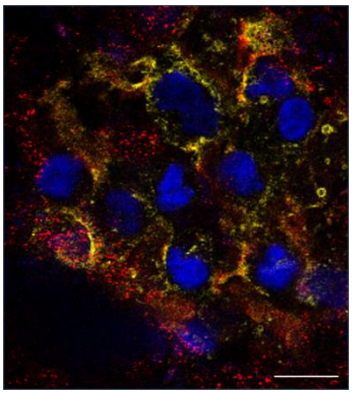

Figure 13 hiPSC-CM survival and attachment in rabbit dECM.
Staining for cells and matrix proteins (laminin, fibronectin, and collagen I) show cells present in the rabbit dECM. Scale bar: 10 μm.

Viability of cells in the rabbit dECM was measured and showed improvement over existing published recellularization data.[13,30] For each cardiac ring immunostained for matrix proteins and nuclei, six representative images were analyzed to quantify the cell number and matrix area. The average cellularity of the characterized rabbit cardiac rings was 63%, relative to the human cadaveric cardiac tissue (Table 4).

Table 4 Viability and cellularity of hiPSC-CMs in rabbit cardiac dECM.

Ring	Cell Number	% Viability	Average % Cellularity
1	648.574	65%	72%
2	521.518	52%	59%
3	558.240	56%	59%

4.3.2. Characterization of Cardiac Rings made with hiPSC-CMs in Rabbit Cardiac dECM

Spontaneous contraction frequency was calculated based on pixel-tracking analysis of video recordings. The number of contractions in a 10-second window was counted and extrapolated to produce an average contraction frequency of 45.68 beats per minute (BPM, Table 5). The video recording was further analyzed to measure tissue displacement for each contraction. Maximum contraction displacement was 54 μm after 7 days.

Table 5 Contractility of hiPSC-CMs in rabbit cardiac dECM.

Ring	Frequency [beats/min]	Maximum Contraction Displacement [microns]
4	50.3	27.04
5	47.8	32.81
6	50	46.66
7	30	36.65
8	60	54.15
9	36	10.57

4.3.3. Spontaneous Electrical Activity

After the cardiac rings were removed from the bioreactor, they were evaluated under a light microscope with 10x objective lens. No visual contractions on the scale of

microns were observed. When the cardiac rings were placed on the MEA for evaluation, spontaneous electrical signals were observed. Cells cultured in 2D on a tissue culture plate were also measured for spontaneous electrical signals to compare against 2D culture. Frequency was increased in all stimulation groups when compared with the non-stim group ($P < 0.0001$, n=6 per group, Figure 14). One statistical outlier in the E/M-Stim group was removed prior to analysis for statistical differences among groups. In addition, the field potential duration (FPD) decreased in the stimulated groups, indicating a faster action potential (Figure 15).[154] Most notably, the non-stim group had the most immature electrophysiological properties observed among the four test groups.

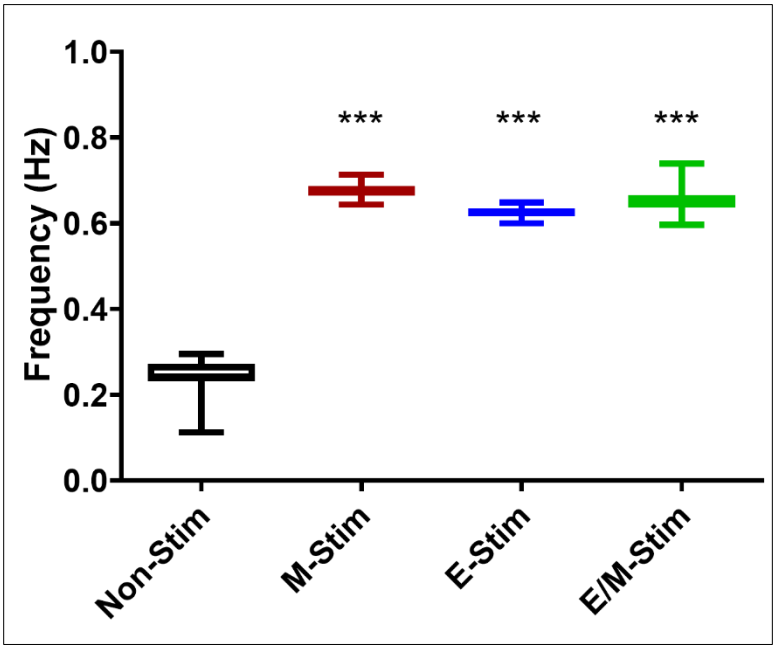

Figure 14 Frequency of electrical signal peaks recorded in cardiac rings.
*** $p < 0.0001$ versus Non-Stim.

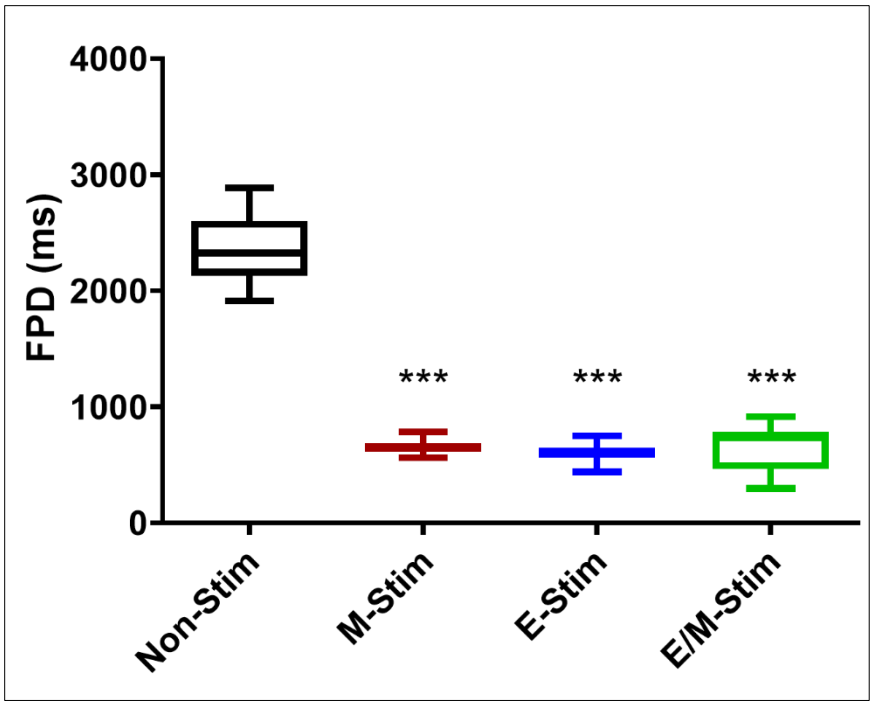

Figure 15 Field potential duration (FPD) recorded in cardiac rings.
*** $p < 0.0001$ versus Non-Stim.

4.3.4. Drug Responsiveness

When dobutamine was applied to stimulate the cardiomyocytes in the cardiac rings, a dose-dependent increase in beat frequency was observed. At the two highest concentrations of dobutamine (166 μM and 1660 μM), a significant increase in the beat rate was observed in the one Non-Stim cardiac ring that was tested (n>62 analyzed peaks in 3 cardiac rings per group, Figure 16).

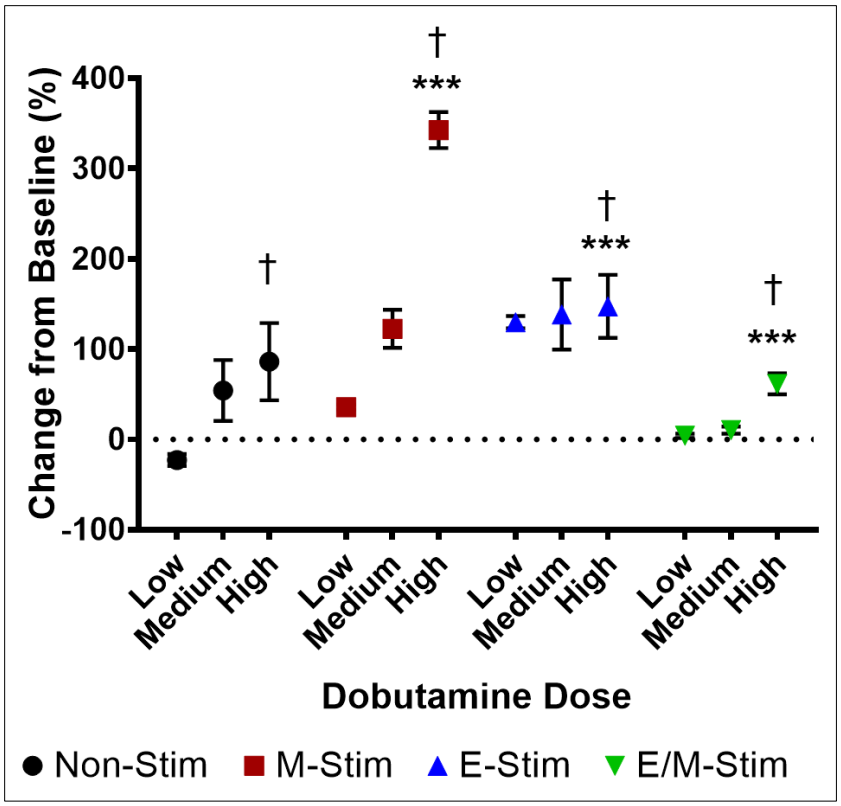

Figure 16 Changes in beat frequency of cardiac rings in response to increasing concentrations of dobutamine.
*** $p < 0.0001$ versus Non-Stim, High dose of dobutamine. † $p < 0.0001$ versus Low dose of dobutamine in same stimulation group.

4.3.5. Structural Maturation

After 7 days in culture, nuclear elongation was quantified using immunostained samples. Images were taken using a Leica SP5 confocal microscope. Images were processed in ImageJ to outline the nuclei and measure the major and minor axes. The elongation of each nucleus was expressed using the ratio of the major to minor axis. The average elongation of cells in the Non-Stim, M-Stim, and E/M-Stim groups were not significantly different (1.781 ± 0.018, n=1107 nuclei in 6 rings, 1.793 ± 0.019 n=935

nuclei in 3 rings, 1.725 ± 0.038, n=311 in 3 rings respectively). Cells in the cardiac rings of the E-Stim group (1.723 ± 0.012, n=2172 in 3 rings) showed an increase in cellular elongation when compared with the Non-Stim and M-Stim cells ($p<0.05$), however the same trend of cellular elongation was not observed when combined electromechanical stimulation was applied to the cardiac rings (Figure 17).

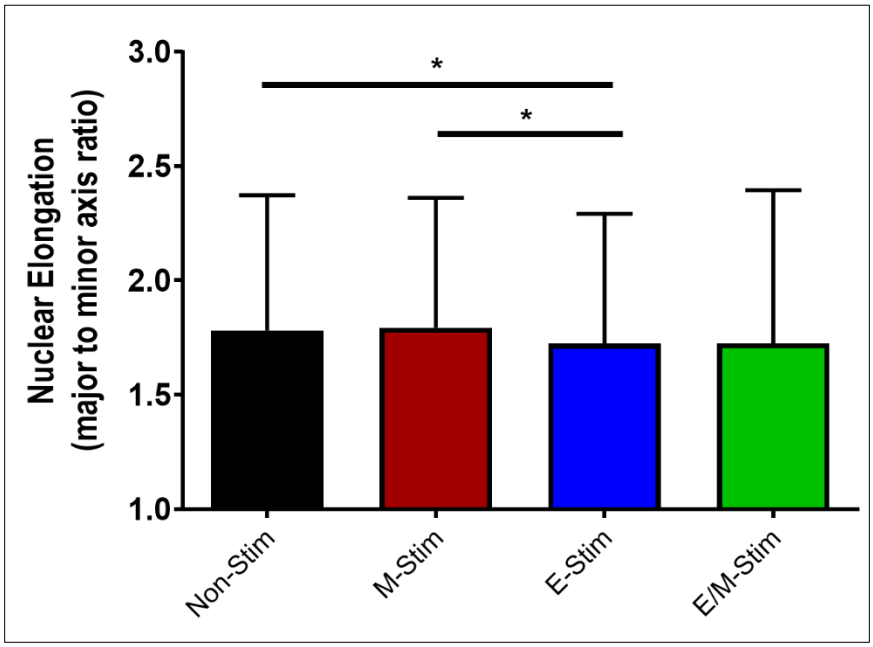

Figure 17 Nuclear elongation of cells in cardiac rings.
*$p<0.05$.

4.4. Discussion

Here, we established a method for creating cardiac rings by recellularizing rabbit cardiac dECM with hiPSC-CMs and showed native-like electrophysiological properties

after 7 days with mechanical and electrical stimulation in a bioreactor. We also observed drug responsiveness to dobutamine in all stimulation groups of cardiac rings.

Building on what we learned in creating cardiac rings with NRCMs in rat cardiac dECM bioscaffolds, we scaled up to using rabbit dECM because rabbit hearts provide a good size model for the pediatric human heart as the hearts are approximately the same size.[155] While previous studies have looked into the function of mouse cardiac cells in cardiac microtissues, human cardiomyocytes have not yet been studied in cardiac dECM scaffolds.[156] The cardiac rings that we created had contraction frequencies observed within human physiologic range (50-115 BPM).[157,158] While frequencies were on the lower end of the physiologic range,[159] studies are already in progress to improve the contraction frequency to be on par with what is observed in an average human (83.9 ± 10.2 BPM).[160] These results also suggest that the cell type may be more important to tissue behavior than the scaffold because the contraction frequency in the constructs were closer to the heart beat range in a human rather than in a rabbit.[161] Existing literature point to some dECM differences in relative protein composition, but ECM from any species seems to be able to help in cardiac regeneration and organization.[162] Interactions between cells and between cells and matrix have been shown to be a critical part of cardiomyocyte maturation and function.[163] For example, integrin has previously been shown to be necessary for maturation,[164] which is consistent with the integrin β1 expression we observed between the cells and matrix.

Being able to improve contraction displacement and frequency is important step in creating functional engineered cardiac tissues. We examined electrophysiologic

maturation of hiPSC-CMs in cardiac dECM rings under uniaxial stretch and electric field stimulation. We showed through the electrical readings of cells in cardiac rings as measured by MEA that stimulation changes the field potential of cardiomyocytes. Cells lost their contractile automaticity, but their beat frequency and field potential duration were driven into human physiologic range. In early 2019, researchers reported using MEAs with atomic force microscopy (AFM) to measure real-time beating force and electric events.[165] Though we did not apply mechanical stretch during MEA recordings, we saw differences between the mechanically-stimulated group and the non-stimulated group, which were consistent with differences observed in cardiomyocytes under real-time stretching. The lasting effects of mechanical stimulation on cardiomyocyte electrical behavior build upon what is already known of uniaxial and biaxial stretch inducing phenotypic changes in cardiomyocytes.[166]

The effects of either electrical or mechanical stimulation appear to drive maturation but do not appear to be synergistic when combined, suggesting that a single stimulation mode, such as mechanical stimulation alone or electrical stimulation alone, is sufficient for improving hiPSC-CM maturation. In previous studies in other labs, combined stimuli have shown mixed results with regards to synergistic effects of electromechanical stimulation on cardiomyocyte maturation and contractility. When timing delays between stimuli were tested, a delay of 0.01 seconds between electrical and mechanical stimulation was found to be optimal for maximizing twitch force but did not have a synergistic effect.[167] We incorporated this timing delay into our bioreactor but did not test different timing delays in order to reduce the combination of various conditions

tested in this study. In porcine cardiac dECM recellularized with mesenchymal stem cells, electromechanical stimulation synergistically increased cellularity of bioscaffold but did not elicit an electrophysiological response in the engineered cardiac tissue constructs, possibly due to low cell density.[150] Our results differed from this previous study by presenting results of spontaneous electrical activity recordings from recellularized cardiac rings, indicating improved cellularity in the tissue-engineered cardiac construct resulting in improved electrophysiological function. Other investigators demonstrated that increasing electrical stimulation intensity without any mechanical stimulation has the greatest effect on maturation, which could be a future direction for our study of cardiac rings since we held the electrical stimulation voltage constant throughout the culture time of the cardiac rings to minimize culture condition variation.[168]

Furthermore, stimulation of cardiac rings resulted in beat frequencies and FPDs that were comparable to what has been previously observed in embryoid bodies.[154] However, we achieved these beat frequencies and FPDs in 7 days, whereas embryoid bodies were cultured for 95 days, demonstrating the impact of electrical and mechanical stimulation on hiPSC-CMs in the dECM environment.[154] This shortened culture time with stimulation can shorten methods for maturing hiPSC-CMs in cardiac constructs and help scientists achieve maturation properties that are more physiologically relevant than what is currently available.[169]

Not only did the cardiac rings display improved electrophysiological maturation after stimulation, but all stimulation groups of cardiac rings showed a physiological response to increased doses of dobutamine, indicating functional adrenergic receptors in

cardiac cells. However, one limitation is the lack of contractility in the cardiac rings. For use in pharmacological studies, contractions may not be needed, but to show full function of cardiac constructs, contractions must be present. These contractions must be sufficient to aid in the pumping of the native heart.[170] Generating functional cardiac tissue that can restore native function remains a challenge for investigators in whole heart tissue engineering, and therefore, scaling up to a whole organ would require that contractility be addressed. A goal of cardiac tissue engineering is to be able to create a function heart as an organ transplant option. We are still working towards increasing the contraction force of engineered cardiac tissue. Including chemical signals, such as tri-iodi-I-thryonine (T3), or adding more cardiomyocytes could be used to address the low contractility in the future.[168]

In conclusion, we observed more mature electrophysiologic characteristics of beat frequency and field potential duration in electrically or mechanically stimulated cardiac rings but did not observe a synergistic response when the two stimuli were combined, suggesting that different combinations of timing delay, voltage, and mechanical stretch could be optimized to promote greater cardiomyocyte maturation.

5. CONCLUSIONS

5.1. Summary

In summary, I tissue engineered cardiac rings using electromechanical stimulation to mature cardiomyocytes in cardiac decellularized extracellular matrix. In Chapter 2, I generated a contracting whole rat heart by using the naturally-derived protein gelatin as a cell delivery vehicle for neonatal rat cardiomyocytes into the decellularized rat heart. In Chapter 3, I characterized cardiac rings made by injecting human induced pluripotent stem cell-derived cardiomyocytes (hiPSC-CMs) into transversely-cut 1mm left ventricular rings of rabbit cardiac decellularized extracellular matrix (dECM). In Chapter 4, I studied the electrophysiological maturation effects of uniaxial stretch and electric field on cardiac rings. Altogether these studies and results provide knowledge and insights into cardiovascular tissue engineering with hiPSC-CMs, dECM bioscaffolds, and biophysical stimulation.

5.2. Significance of Work

Every year, more than 17 million people worldwide die of cardiovascular disease (CVD).[171] In the United States (US) alone, CVD has been the leading cause of adult deaths for more than fifty years.[172] While significant progress has been made to prevent and treat CVD, many patients still suffer from long-term CVD, eventually requiring heart transplants. With more than 4,000 individuals in the US waiting for a donor heart based on Organ Procurement and Transplantation Network (OPTN) data as of April 20, 2019, the shortage of organ donors is evident. The gap between the number of those waiting for

a heart and the number of hearts available continues to grow.[173] Patients and their families feel the deep need for alternative therapies as they wait for a donor heart to become available.[174] Cardiovascular tissue engineering aims to address this need by engineering hearts for patients.

One approach to cardiovascular tissue engineering is the decellularization and recellularization of the heart. The recellularization of decellularized organs with recipient-specific cells decreases the need for immunosuppressants and the risk of organ rejection.[175] In addition, this process allows hearts that are normally not immunocompatible with the patient to be considered for transplantation.[176] Decellularized hearts may also increase organ availability by converting a non-transplantable heart into a patient-specific heart ready for transplant.[177]

The results in this dissertation are significant to the field of cardiovascular tissue engineering because we have progressed from using neonatal rat cardiomyocytes in rat cardiac dECM bioscaffolds to human cardiomyocytes in pediatric human-sized cardiac rings. Scaling up from primary cells to human stem cell-derived cardiomyocytes allows us to generate more cardiomyocytes given the self-renewal of the hiPSCs. Since we are now using human cells in tissue constructs, we could potentially translate findings to clinical applications.[178]

In addition, the cardiomyocytes in the cardiac dECM matrix under electrical and mechanical stimulation appear more mature than cardiomyocytes in two-dimensional cell culture given the same amount of time in cell culture. The implications of this improved maturation would allow research scientists to save time and resources while driving

maturation in hiPSC-CMs. The findings of studies using mature hiPSC-CMs are more relevant to the clinical setting because the cardiomyocytes found in the human body behave very differently from immature hiPSC-CMs.[179] Engineering a bioartificial heart as a transplant option for patients calls for cells that will be comparable to those found in the body, and achieving greater maturation is less amount of time will help us achieve this goal.

5.3. Future Directions

Despite the advancements from this study and others, creating heart tissue on an organ-scale is still a looming challenge. In using the cardiac dECM, the number of CMs needed in recellularization is not the only hurdle; getting the proper milieu of cell types that drives function in the heart is also necessary.[180,181] Since we are conducting these experiments ex vivo, we must be able to culture different cell types together in one construct, with the bioactive dECM bioscaffold providing the necessary cues for cell organization and function.[182]

Another field in which development is promising is in the bioreactor technology needed for creating bioartificial heart tissue and organs.[183] The results of electromechanical stimulation in cardiac tissue are promising for the field of cardiovascular tissue engineering. Not only do the results from our studies lead to increased knowledge about which electrophysiological properties of hiPSC-CMs can be improved, but also this knowledge can be used practically to decrease the culture time needed to make these cardiac tissues and constructs. As more labs look into recellularizing

and growing hearts, we hope that scientists and engineers continue to develop the whole-organ bioreactors that are needed to culture these organs.

Once the whole heart has been recellularized and stimulated to achieve greater cardiomyocyte maturation, its function should be evaluated in vivo. Studies that include heterotopic animal transplants provide researchers with an opportunity to study the engineered organ under physiologic conditions.[184] Acute endpoints such as thrombosis and contractility show the feasibility of the construct in the animal, while long-term studies provide the foundation to prove viability and durability in preclinical studies[185]. These in vivo tests would be an important next step in engineering a whole bioartificial heart.

Beyond in vivo testing, tissue-engineered heart constructs can also be used for disease modeling and drug testing.[186] With the creation of disease specific hiPSC-CMs and CRISPR-Cas9 systems in place, patient-specific cardiac constructs can be made to predict how drugs will affect certain patient populations.[187] These studies would be the next steps in engineering cardiac tissues to be used in new technologies, such as organs-on-a-chip.

Altogether, the field of cardiovascular tissue engineering is ever-changing and developing with new technologies being used, created, and perfected. As discussed, this dissertation aims to shed light on a few aspects in the field of cardiovascular tissue engineering with hiPSC-CMs, dECM bioscaffolds, and electromechanical bioreactors.

REFERENCES

1 Kassebaum, N. J. *et al.* Global, regional, and national disability-adjusted life-years (DALYs) for 315 diseases and injuries and healthy life expectancy (HALE), 1990–2015: a systematic analysis for the Global Burden of Disease Study 2015. *The Lancet* **388**, 1603-1658 (2016).

2 Wang, H. *et al.* Global, regional, and national life expectancy, all-cause mortality, and cause-specific mortality for 249 causes of death, 1980–2015: a systematic analysis for the Global Burden of Disease Study 2015. *The lancet* **388**, 1459-1544 (2016).

3 Cohn, J. N. Heart failure in 2013: continue what we are doing to treat HF, but do it better. *Nature Reviews. Cardiology* **11**, 69 (2014).

4 Yancy, C. W. *et al.* 2017 ACC/AHA/HFSA focused update of the 2013 ACCF/AHA guideline for the management of heart failure: a report of the American College of Cardiology/American Heart Association Task Force on Clinical Practice Guidelines and the Heart Failure Society of America. *Journal of the American College of Cardiology* **70**, 776-803 (2017).

5 Wilhelm, M. J. Long-term outcome following heart transplantation: current perspective. *Journal of thoracic disease* **7**, 549 (2015).

6 Longnus, S. L. *et al.* Heart transplantation with donation after circulatory determination of death. *Nature Reviews Cardiology* **11**, 354 (2014).

7 Schmuck, E. G., Hematti, P. & Raval, A. N. *Cardiac Extracellular Matrix: Fundamental Science to Clinical Applications*. Vol. 1098 (Springer, 2018).

8 Shalak, R. & Fox, C. Tissue Engineering: Proceedings for a Workshop Held at Granlibakken, Lake Tahoe, California, February 26–29. *New York: Alan Liss* (1988).

9 Langer, R. & Vacanti, J. Tissue engineering. *Science* **260**, 920-926, doi:10.1126/science.8493529 (1993).

10 Matsa, E., Burridge, P. W. & Wu, J. C. Human Stem Cells for Modeling Heart Disease and for Drug Discovery. *Science Translational Medicine* **6**, 239ps236-239ps236, doi:10.1126/scitranslmed.3008921 (2014).

11 Wang, B. *et al.* Establishing Early Functional Perfusion and Structure in Tissue Engineered Cardiac Constructs. *Critical Reviews™ in Biomedical Engineering* **43** (2015).

12 Kaiser, N. J. & Coulombe, K. L. Physiologically inspired cardiac scaffolds for tailored in vivo function and heart regeneration. *Biomedical Materials* **10**, 034003 (2015).

13 Ott, H. C. *et al.* Perfusion-decellularized matrix: using nature's platform to engineer a bioartificial heart. *Nat Med* **14**, 213-221, doi:10.1038/nm1684 (2008).

14 Guyette, J. P. *et al.* Bioengineering human myocardium on native extracellular matrixnovelty and significance. *Circulation research* **118**, 56-72 (2016).

15 Hodgson, M. J., Knutson, C. C., Momtahan, N. & Cook, A. D. Extracellular matrix from whole porcine heart decellularization for cardiac tissue engineering. *Methods in Molecular Biology*, 1-8 (2017).

16 Kitahara, H. *et al.* Heterotopic transplantation of a decellularized and recellularized whole porcine heart. *Interactive cardiovascular and thoracic surgery* **22**, 571-579 (2016).

17 Rieder, E. *et al.* Decellularization protocols of porcine heart valves differ importantly in efficiency of cell removal and susceptibility of the matrix to recellularization with human vascular cells. *The Journal of thoracic and cardiovascular surgery* **127**, 399-405 (2004).

18 Courtman, D. W. *et al.* Development of a pericardial acellular matrix biomaterial: biochemical and mechanical effects of cell extraction. *Journal of biomedical materials research* **28**, 655-666 (1994).

19 Grauss, R. W. *et al.* Histological evaluation of decellularised porcine aortic valves: matrix changes due to different decellularisation methods. *European journal of cardio-thoracic surgery* **27**, 566-571 (2005).

20 Wainwright, J. M. *et al.* Preparation of cardiac extracellular matrix from an intact porcine heart. *Tissue Engineering Part C: Methods* **16**, 525-532 (2009).

21 Robertson, M. J., Dries-Devlin, J. L., Kren, S. M., Burchfield, J. S. & Taylor, D. A. Optimizing recellularization of whole decellularized heart extracellular matrix. *PloS one* **9**, e90406 (2014).

22 Lee, P.-F. *et al.* Inverted orientation improves decellularization of whole porcine hearts. *Acta Biomaterialia* **49**, 181-191, doi:https://doi.org/10.1016/j.actbio.2016.11.047 (2017).

23 Crapo, P. M., Gilbert, T. W. & Badylak, S. F. An overview of tissue and whole organ decellularization processes. *Biomaterials* **32**, 3233-3243 (2011).

24 Garreta, E. *et al.* Tissue engineering by decellularization and 3D bioprinting. *Materials Today* **20**, 166-178 (2017).

25 Ng, S. L., Narayanan, K., Gao, S. & Wan, A. C. Lineage restricted progenitors for the repopulation of decellularized heart. *Biomaterials* **32**, 7571-7580 (2011).

26 Weymann, A. *et al.* Bioartificial heart: a human-sized porcine model–the way ahead. *PloS one* **9**, e111591 (2014).

27 Sánchez, P. L. *et al.* Acellular human heart matrix: A critical step toward whole heart grafts. *Biomaterials* **61**, 279-289, doi:https://doi.org/10.1016/j.biomaterials.2015.04.056 (2015).

28 Guyette, J. P. *et al.* Bioengineering human myocardium on native extracellular matrix. *Circulation research* **118**, 56-72, doi:10.1161/CIRCRESAHA.115.306874 (2016).

29 Ferng, A. S. *et al.* Acellular porcine heart matrices: whole organ decellularization with 3D-bioscaffold & vascular preservation. *Journal of clinical and translational research* **3**, 260 (2017).

30 Lu, T.-Y. *et al.* Repopulation of decellularized mouse heart with human induced pluripotent stem cell-derived cardiovascular progenitor cells. *Nature communications* **4**, 2307 (2013).

31 Hülsmann, J. *et al.* A novel customizable modular bioreactor system for whole-heart cultivation under controlled 3D biomechanical stimulation. *Journal of Artificial Organs* **16**, 294-304, doi:10.1007/s10047-013-0705-5 (2013).

32 Aubin, H., Kranz, A., Hülsmann, J., Lichtenberg, A. & Akhyari, P. in *Cellular Cardiomyoplasty* 163-178 (Springer, 2013).

33 Methe, K. *et al.* An alternative approach to decellularize whole porcine heart. *BioResearch open access* **3**, 327-338 (2014).

34 Momtahan, N. *et al.* Automation of pressure control improves whole porcine heart decellularization. *Tissue Engineering Part C: Methods* **21**, 1148-1161 (2015).

35 Remlinger, N. T., Wearden, P. D. & Gilbert, T. W. Procedure for decellularization of porcine heart by retrograde coronary perfusion. *JoVE (Journal of Visualized Experiments)*, e50059 (2012).

36 Merna, N., Robertson, C., La, A. & George, S. C. Optical imaging predicts mechanical properties during decellularization of cardiac tissue. *Tissue Engineering Part C: Methods* **19**, 802-809 (2013).

37 Zhou, P. & Pu, W. T. (Am Heart Assoc, 2016).

38 Pinto, A. R. *et al.* Revisiting cardiac cellular composition. *Circulation research* **118**, 400-409 (2016).

39 Bergmann, O. *et al.* Dynamics of cell generation and turnover in the human heart. *Cell* **161**, 1566-1575 (2015).

40 Garreta, E. *et al.* Myocardial commitment from human pluripotent stem cells: Rapid production of human heart grafts. *Biomaterials* **98**, 64-78 (2016).

41 Crawford, B. *et al.* Cardiac decellularisation with long ‐ term storage and repopulation with canine peripheral blood progenitor cells. *The Canadian Journal of Chemical Engineering* **90**, 1457-1464 (2012).

42 Yasui, H. *et al.* Excitation propagation in three-dimensional engineered hearts using decellularized extracellular matrix. *Biomaterials* **35**, 7839-7850, doi:http://dx.doi.org/10.1016/j.biomaterials.2014.05.080 (2014).

43 Yasui, H. *et al.* Excitation propagation in three-dimensional engineered hearts using decellularized extracellular matrix. *Biomaterials* **35**, 7839-7850 (2014).

44 Narmoneva, D. A., Vukmirovic, R., Davis, M. E., Kamm, R. D. & Lee, R. T. Endothelial cells promote cardiac myocyte survival and spatial reorganization: implications for cardiac regeneration. *Circulation* **110**, 962-968 (2004).

45 Zhang, J. *et al.* Functional cardiomyocytes derived from human induced pluripotent stem cells. *Circulation research* **104**, e30-e41 (2009).

46 Narsinh, K., Narsinh, K. H. & Wu, J. C. Derivation of Induced Pluripotent Stem Cells for Human Disease Modeling. *Circulation research* **108**, 10.1161/CIRCRESAHA.1111.240374, doi:10.1161/CIRCRESAHA.111.240374 (2011).

47 Inoue, H. & Yamanaka, S. The Use of Induced Pluripotent Stem Cells in Drug Development. *Clinical Pharmacology & Therapeutics* **89**, 655-661, doi:doi:10.1038/clpt.2011.38 (2011).

48 Itzhaki, I. *et al.* Modelling the long QT syndrome with induced pluripotent stem cells. *Nature* **471**, 225 (2011).

49 Bergmann, O. *et al.* Evidence for Cardiomyocyte Renewal in Humans. *Science* **324**, 98-102, doi:10.1126/science.1164680 (2009).

50 Yang, X., Pabon, L. & Murry, C. E. Engineering adolescence: maturation of human pluripotent stem cell–derived cardiomyocytes. *Circulation research* **114**, 511-523 (2014).

51 Drouin, E., Charpentier, F., Gauthier, C., Laurent, K. & Le Marec, H. Electrophysiologic characteristics of cells spanning the left ventricular wall of human heart: evidence for presence of M cells. *Journal of the American College of Cardiology* **26**, 185-192 (1995).

52 Kim, C. *et al.* Non-Cardiomyocytes Influence the Electrophysiological Maturation of Human Embryonic Stem Cell-Derived Cardiomyocytes During Differentiation. *Stem Cells and Development* **19**, 783-795, doi:10.1089/scd.2009.0349 (2010).

53 Keung, W., Boheler, K. R. & Li, R. A. Developmental cues for the maturation of metabolic, electrophysiological and calcium handling properties of human pluripotent stem cell-derived cardiomyocytes. *Stem cell research & therapy* **5**, 17 (2014).

54 Lundy, S. D., Zhu, W.-Z., Regnier, M. & Laflamme, M. A. Structural and functional maturation of cardiomyocytes derived from human pluripotent stem cells. *Stem cells and development* **22**, 1991-2002 (2013).

55 Robertson, C., Tran, D. D. & George, S. C. Concise Review: Maturation Phases of Human Pluripotent Stem Cell-Derived Cardiomyocytes. *Stem cells (Dayton, Ohio)* **31**, 10.1002/stem.1331, doi:10.1002/stem.1331 (2013).

56 Kamakura, T. *et al.* Ultrastructural maturation of human-induced pluripotent stem cell-derived cardiomyocytes in a long-term culture. *Circulation Journal* **77**, 1307-1314 (2013).

57 Feric, N. T. & Radisic, M. Towards adult-like human engineered cardiac tissue: Maturing human pluripotent stem cell-derived cardiomyocytes in human engineered cardiac tissues. *Advanced drug delivery reviews* **96**, 110-134, doi:10.1016/j.addr.2015.04.019 (2016).

58 Tandon, N. *et al.* Electrical stimulation systems for cardiac tissue engineering. *Nature protocols* **4**, 155 (2009).

59 Hirt, M. N. *et al.* Functional improvement and maturation of rat and human engineered heart tissue by chronic electrical stimulation. *Journal of molecular and cellular cardiology* **74**, 151-161 (2014).

60 Zimmermann, W.-H. *et al.* Tissue engineering of a differentiated cardiac muscle construct. *Circulation research* **90**, 223-230 (2002).

61 Baharvand, H., Azarnia, M., Parivar, K. & Ashtiani, S. K. The effect of extracellular matrix on embryonic stem cell-derived cardiomyocytes. *Journal of molecular and cellular cardiology* **38**, 495-503 (2005).

62 Nunes, S. S. *et al.* Biowire: a platform for maturation of human pluripotent stem cell–derived cardiomyocytes. *Nature methods* **10**, 781 (2013).

63 Lieu, D. K. *et al.* Absence of transverse tubules contributes to non-uniform ca2+ wavefronts in mouse and human embryonic stem cell–derived cardiomyocytes. *Stem cells and development* **18**, 1493-1500 (2009).

64 Shimko, V. F. & Claycomb, W. C. Effect of Mechanical Loading on Three-Dimensional Cultures of Embryonic Stem Cell-Derived Cardiomyocytes. *Tissue engineering. Part A* **14**, 49-58, doi:10.1089/ten.2007.0092 (2008).

65 Zimmermann, W.-H. *et al.* Engineered heart tissue grafts improve systolic and diastolic function in infarcted rat hearts. *Nat Med* **12**, 452-458, doi:http://www.nature.com/nm/journal/v12/n4/suppinfo/nm1394_S1.html (2006).

66 Vuong, J. T. *et al.* Mortality From Heart Failure and Dementia in the United States: CDC WONDER 1999–2016. *Journal of Cardiac Failure* **25**, 125-129, doi:https://doi.org/10.1016/j.cardfail.2018.11.012 (2019).

67 Zannad, F. Rising incidence of heart failure demands action. *The Lancet* **391**, 518-519, doi:https://doi.org/10.1016/S0140-6736(17)32873-8 (2018).

68 Khush, K. K. *et al.* The International Thoracic Organ Transplant Registry of the International Society for Heart and Lung Transplantation: Thirty-fifth Adult Heart Transplantation Report—2018; Focus Theme: Multiorgan Transplantation. *The Journal of Heart and Lung Transplantation* **37**, 1155-1168, doi:https://doi.org/10.1016/j.healun.2018.07.022 (2018).

69 Heidenreich, P. A. *et al.* Forecasting the Impact of Heart Failure in the United States. *Circulation: Heart Failure* **6**, 606-619, doi:doi:10.1161/HHF.0b013e318291329a (2013).

70 Langer, R. S. & Vacanti, J. P. Tissue engineering: the challenges ahead. *Sci Am* **280**, 86-89 (1999).

71 Badylak, S. F., Taylor, D. & Uygun, K. Whole-organ tissue engineering: decellularization and recellularization of three-dimensional matrix scaffolds.

Annu. Rev. Biomed. Eng. **13**, 27-53, doi:10.1146/annurev-bioeng-071910-124743 (2011).

72 Kitahara, H. *et al.* Heterotopic transplantation of a decellularized and recellularized whole porcine heart†. *Interactive CardioVascular and Thoracic Surgery* **22**, 571-579, doi:10.1093/icvts/ivw022 (2016).

73 Guyette, J. P. *et al.* Bioengineering human myocardium on native extracellular matrix. *Circ. Res.* **118**, 56-72, doi:10.1161/CIRCRESAHA.115.306874 (2016).

74 Tirziu, D., Giordano, F. J. & Simons, M. Cell Communications in the Heart. *Circulation* **122**, 928-937, doi:doi:10.1161/CIRCULATIONAHA.108.847731 (2010).

75 Gobin, A. S., Taylor, D. A., Chau, E. & Sampaio, L. C. in *Stem Cell and Gene Therapy for Cardiovascular Disease* (eds Emerson C. Perin, Leslie W. Miller, Doris A. Taylor, & James T. Willerson) 349-373 (Academic Press, 2016).

76 Uygun, B. E., Yarmush, M. L. & Uygun, K. Application of whole-organ tissue engineering in hepatology. *Nat. Rev. Gastroenterol. Hepatol.* **9**, 738, doi:10.1038/nrgastro.2012.140 (2012).

77 Malavolta, M. *et al.* Changes in Zn homeostasis during long term culture of primary endothelial cells and effects of Zn on endothelial cell senescence. *Experimental Gerontology* **99**, 35-45, doi:https://doi.org/10.1016/j.exger.2017.09.006 (2017).

78 Pi, L. *et al.* Connective tissue growth factor with a novel fibronectin binding site promotes cell adhesion and migration during rat oval cell activation. *Hepatology* **47**, 996-1004, doi:10.1002/hep.22079 (2008).

79 Kido, K., Ito, H., Yamamoto, Y., Makita, K. & Uchida, T. Cytotoxicity of propofol in human induced pluripotent stem cell-derived cardiomyocytes. *Journal of anesthesia* **32**, 120-131 (2018).

80 Duriez, P. J., Wong, F., Dorovini-Zis, K., Shahidi, R. & Karsan, A. A1 functions at the mitochondria to delay endothelial apoptosis in response to tumor necrosis factor. *Journal of Biological Chemistry* **275**, 18099-18107 (2000).

81 Voytik-Harbin, S. L., Rajwa, B. & Robinson, J. P. Three-dimensional imaging of extracellular matrix and extracellular matrix-cell interactions. *Methods in cell biology* **63**, 583-597 (2001).

82 Onaizah, O., Poepping, T. L. & Zamir, M. A model of blood supply to the brain via the carotid arteries: Effects of obstructive vs. sclerotic changes. *Medical*

Engineering & Physics **49**, 121-130, doi:https://doi.org/10.1016/j.medengphy.2017.08.009 (2017).

83 Conklin, B. S., Wu, H., Lin, P. H., Lumsden, A. B. & Chen, C. Basic Fibroblast Growth Factor Coating and Endothelial Cell Seeding of a Decellularized Heparin-coated Vascular Graft. *Artificial Organs* **28**, 668-675, doi:10.1111/j.1525-1594.2004.00062.x (2004).

84 Nezhadi, S. H., Choong, P. F., Lotfipour, F. & Dass, C. R. Gelatin-based delivery systems for cancer gene therapy. *Journal of drug targeting* **17**, 731-738 (2009).

85 Santoro, M., Tatara, A. M. & Mikos, A. G. Gelatin carriers for drug and cell delivery in tissue engineering. *Journal of Controlled Release* **190**, 210-218, doi:https://doi.org/10.1016/j.jconrel.2014.04.014 (2014).

86 Vandelli, M. A., Rivasi, F., Guerra, P., Forni, F. & Arletti, R. Gelatin microspheres crosslinked with d,l-glyceraldehyde as a potential drug delivery system: preparation, characterisation, in vitro and in vivo studies. *International Journal of Pharmaceutics* **215**, 175-184, doi:https://doi.org/10.1016/S0378-5173(00)00681-5 (2001).

87 Jiankang, H. *et al.* Preparation of chitosan–gelatin hybrid scaffolds with well-organized microstructures for hepatic tissue engineering. *Acta biomaterialia* **5**, 453-461 (2009).

88 Rathna, G. V. N. Gelatin hydrogels: enhanced biocompatibility, drug release and cell viability. *Journal of Materials Science: Materials in Medicine* **19**, 2351-2358, doi:10.1007/s10856-007-3334-9 (2008).

89 Gómez-Guillén, M., Giménez, B., López-Caballero, M. a. & Montero, M. Functional and bioactive properties of collagen and gelatin from alternative sources: A review. *Food hydrocolloids* **25**, 1813-1827 (2011).

90 Van Luyn, M., Van Wachem, P., Dijkstra, P., Damink, L. O. & Feijen, J. Calcification of subcutaneously implanted collagens in relation to cytotoxicity, cellular interactions and crosslinking. *Journal of Materials Science: Materials in Medicine* **6**, 288-296 (1995).

91 Kuwahara, K., Yang, Z., Slack, G. C., Nimni, M. E. & Han, B. Cell Delivery Using an Injectable and Adhesive Transglutaminase–Gelatin Gel. *Tissue Engineering Part C: Methods* **16**, 609-618, doi:10.1089/ten.tec.2009.0406 (2010).

92 Shu, X. Z., Liu, Y., Palumbo, F. S., Luo, Y. & Prestwich, G. D. In situ crosslinkable hyaluronan hydrogels for tissue engineering. *Biomaterials* **25**, 1339-1348 (2004).

93 Schwick, H. & Heide, K. Immunochemistry and immunology of collagen and gelatin. *Bibliotheca Haematologica* **33**, 111-125 (1969).

94 Courts, A. & Ward, A. G. *The science and technology of gelatin*. (Academic Press, 1977).

95 Mladenovska, K., Kumbaradzi, E., Dodov, G., Makraduli, L. & Goracinova, K. Biodegradation and drug release studies of BSA loaded gelatin microspheres. *International journal of pharmaceutics* **242**, 247-249 (2002).

96 Kozlov, P. & Burdygina, G. The structure and properties of solid gelatin and the principles of their modification. *Polymer* **24**, 651-666 (1983).

97 Lai, J.-Y., Li, Y.-T., Cho, C.-H. & Yu, T.-C. Nanoscale modification of porous gelatin scaffolds with chondroitin sulfate for corneal stromal tissue engineering. *International journal of nanomedicine* **7**, 1101-1114, doi:10.2147/IJN.S28753 (2012).

98 Hsiue, G.-H., Lai, J.-Y., Chen, K.-H. & Hsu, W.-M. A novel strategy for corneal endothelial reconstruction with a bioengineered cell sheet. *Transplantation* **81**, 473-476 (2006).

99 Rose, J. *et al.* Gelatin-based materials in ocular tissue engineering. *Materials* **7**, 3106-3135 (2014).

100 Okamoto, T. *et al.* Cartilage regeneration using slow release of bone morphogenetic protein-2 from a gelatin sponge to treat experimental canine tracheomalacia: a preliminary report. *ASAIO journal* **49**, 63-69 (2003).

101 Hoshikawa, A. *et al.* Encapsulation of chondrocytes in photopolymerizable styrenated gelatin for cartilage tissue engineering. *Tissue engineering* **12**, 2333-2341 (2006).

102 Bronshtein, T. *et al.* A mathematical model for analyzing the elasticity, viscosity, and failure of soft tissue: Comparison of native and decellularized porcine cardiac extracellular matrix for tissue engineering. *Tissue Eng. Part C Methods* **19**, 620-630, doi:10.1089/ten.tec.2012.0387 (2013).

103 Hoganson, D. M. *et al.* Preserved extracellular matrix components and retained biological activity in decellularized porcine mesothelium. *Biomaterials* **31**, 6934-6940, doi:https://doi.org/10.1016/j.biomaterials.2010.05.026 (2010).

104 Esmaeili Pourfarhangi, K., Mashayekhan, S., Asl, S. G. & Hajebrahimi, Z. Construction of scaffolds composed of acellular cardiac extracellular matrix for myocardial tissue engineering. *Biologicals* **53**, 10-18, doi:https://doi.org/10.1016/j.biologicals.2018.03.005 (2018).

105 Faulk, D. M., Johnson, S. A., Zhang, L. & Badylak, S. F. Role of the extracellular matrix in whole organ engineering. *J. Cell. Physiol.* **229**, 984-989, doi:10.1002/jcp.24532 (2014).

106 Zhang, Y. S. *et al.* From cardiac tissue engineering to heart-on-a-chip: beating challenges. *Biomedical Materials* **10**, 034006 (2015).

107 Zimmermann, W.-h. H., DE), Eschenhagen, Thomas (Hamburg, DE). Multiloop Engineered Heart Muscle Tissue. United States patent (2019).

108 Stainsby, G. Viscosity of Dilute Gelatin Solutions. *Nature* **169**, 662, doi:10.1038/169662a0 (1952).

109 Flory, P. J. & Garrett, R. R. Phase transitions in collagen and gelatin Systems1. *Journal of the American Chemical Society* **80**, 4836-4845 (1958).

110 Artoli, A. M., Sequeira, A., Silva-Herdade, A. S. & Saldanha, C. Leukocytes rolling and recruitment by endothelial cells: hemorheological experiments and numerical simulations. *J Biomech* **40**, 3493-3502, doi:10.1016/j.jbiomech.2007.05.031 (2007).

111 Katagiri, Y., Brew, S. A. & Ingham, K. C. All six modules of the gelatin-binding domain of fibronectin are required for full affinity. *Journal of Biological Chemistry* **278**, 11897-11902 (2003).

112 Yuan, J., Melder, R. J., Jain, R. K. & Munn, L. L. Lateral view flow system for studies of cell adhesion and deformation under flow conditions. *Biotechniques* **30**, 388-394 (2001).

113 Olivier, L. A. & Truskey, G. A. A numerical analysis of forces exerted by laminar flow on spreading cells in a parallel plate flow chamber assay. *Biotechnol Bioeng* **42**, 963-973, doi:10.1002/bit.260420807 (1993).

114 Jadhav, S., Eggleton, C. D. & Konstantopoulos, K. A 3-D computational model predicts that cell deformation affects selectin-mediated leukocyte rolling. *Biophys J* **88**, 96-104, doi:10.1529/biophysj.104.051029 (2005).

115 Oshibe, T., Hayase, T., Funamoto, K. & Shirai, A. Numerical analysis for elucidation of nonlinear frictional characteristics of a deformed erythrocyte

moving on a plate in medium subject to inclined centrifugal force. *J Biomech Eng* **136**, 121003, doi:10.1115/1.4028723 (2014).

116 McCue, S., Noria, S. & Langille, B. L. Shear-induced reorganization of endothelial cell cytoskeleton and adhesion complexes. *Trends Cardiovasc Med* **14**, 143-151, doi:10.1016/j.tcm.2004.02.003 (2004).

117 Langille, B. L. Morphologic responses of endothelium to shear stress: reorganization of the adherens junction. *Microcirculation* **8**, 195-206, doi:10.1038/sj/mn/7800085 (2001).

118 Olesen, S. P., Clapham, D. E. & Davies, P. F. Haemodynamic shear stress activates a K+ current in vascular endothelial cells. *Nature* **331**, 168-170, doi:10.1038/331168a0 (1988).

119 Chen, K. D. *et al.* Mechanotransduction in response to shear stress. Roles of receptor tyrosine kinases, integrins, and Shc. *J Biol Chem* **274**, 18393-18400 (1999).

120 Tzima, E., del Pozo, M. A., Shattil, S. J., Chien, S. & Schwartz, M. A. Activation of integrins in endothelial cells by fluid shear stress mediates Rho-dependent cytoskeletal alignment. *EMBO J* **20**, 4639-4647, doi:10.1093/emboj/20.17.4639 (2001).

121 Kutschka, I. *et al.* Collagen matrices enhance survival of transplanted cardiomyoblasts and contribute to functional improvement of ischemic rat hearts. *Circulation* **114**, I167-173, doi:10.1161/CIRCULATIONAHA.105.001297 (2006).

122 Roche, E. T. *et al.* Comparison of biomaterial delivery vehicles for improving acute retention of stem cells in the infarcted heart. *Biomaterials* **35**, 6850-6858, doi:10.1016/j.biomaterials.2014.04.114 (2014).

123 Feinberg, A. W. *et al.* Controlling the contractile strength of engineered cardiac muscle by hierarchal tissue architecture. *Biomaterials* **33**, 5732-5741 (2012).

124 Pope, A. J., Sands, G. B., Smaill, B. H. & LeGrice, I. J. Three-dimensional transmural organization of perimysial collagen in the heart. *American Journal of Physiology-Heart and Circulatory Physiology* (2008).

125 LeGrice, I. J. *et al.* Laminar structure of the heart: ventricular myocyte arrangement and connective tissue architecture in the dog. *American Journal of Physiology-Heart and Circulatory Physiology* **269**, H571-H582 (1995).

126 Gilbert, S. H., Benson, A. P., Li, P. & Holden, A. V. in *International Conference on Functional Imaging and Modeling of the Heart*. 403-412 (Springer).

127 Mekkaoui, C. *et al.* Diffusion MRI tractography of the developing human fetal heart. *PLoS One* **8**, e72795 (2013).

128 Aubin, H. *et al.* Directed 3D cell alignment and elongation in microengineered hydrogels. *Biomaterials* **31**, 6941-6951, doi:https://doi.org/10.1016/j.biomaterials.2010.05.056 (2010).

129 Salick, M. R. *et al.* Micropattern width dependent sarcomere development in human ESC-derived cardiomyocytes. *Biomaterials* **35**, 4454-4464, doi:https://doi.org/10.1016/j.biomaterials.2014.02.001 (2014).

130 Carson, D. *et al.* Nanotopography-Induced Structural Anisotropy and Sarcomere Development in Human Cardiomyocytes Derived from Induced Pluripotent Stem Cells. *ACS Applied Materials & Interfaces* **8**, 21923-21932, doi:10.1021/acsami.5b11671 (2016).

131 Weidenhamer, N. K., Moore, D. L., Lobo, F. L., Klair, N. T. & Tranquillo, R. T. Influence of culture conditions and extracellular matrix alignment on human mesenchymal stem cells invasion into decellularized engineered tissues. *Journal of tissue engineering and regenerative medicine* **9**, 605-618 (2015).

132 Fu, J., Gao, J., Pi, R. & Liu, P. An optimized protocol for culture of cardiomyocyte from neonatal rat. *Cytotechnology* **49**, 109-116 (2005).

133 Christian, W., Esquembre, F. & Barbato, L. Open source physics. *Science* **334**, 1077-1078 (2011).

134 Wan, C., Frohlich, E., Charest, J. & Kamm, R. Effect of surface patterning and presence of collagen I on the phenotypic changes of embryonic stem cell derived cardiomyocytes. *Cellular and molecular bioengineering* **4**, 56-66 (2011).

135 Tijore, A. *et al.* Contact guidance for cardiac tissue engineering using 3D bioprinted gelatin patterned hydrogel. *Biofabrication* **10**, 025003 (2018).

136 Wang, P.-Y., Yu, J., Lin, J.-H. & Tsai, W.-B. Modulation of alignment, elongation and contraction of cardiomyocytes through a combination of nanotopography and rigidity of substrates. *Acta biomaterialia* **7**, 3285-3293 (2011).

137 Liu, Y. *et al.* Tuning the conductivity and inner structure of electrospun fibers to promote cardiomyocyte elongation and synchronous beating. *Materials Science and Engineering: C* **69**, 865-874 (2016).

138 Taylor, D. A., Sampaio, L. C., Ferdous, Z., Gobin, A. S. & Taite, L. J. Decellularized matrices in regenerative medicine. *Acta Biomaterialia* **74**, 74-89, doi:https://doi.org/10.1016/j.actbio.2018.04.044 (2018).

139 Auman, H. J. *et al.* Functional modulation of cardiac form through regionally confined cell shape changes. *PLoS biology* **5**, e53 (2007).

140 Ribeiro, A. J. *et al.* Contractility of single cardiomyocytes differentiated from pluripotent stem cells depends on physiological shape and substrate stiffness. *Proceedings of the National Academy of Sciences* **112**, 12705-12710 (2015).

141 Ribeiro, A. J. S. *et al.* Contractility of single cardiomyocytes differentiated from pluripotent stem cells depends on physiological shape and substrate stiffness. *Proceedings of the National Academy of Sciences of the United States of America* **112**, 12705-12710, doi:10.1073/pnas.1508073112 (2015).

142 Zheng, C.-X. *et al.* Reconstruction of structure and function in tissue engineering of solid organs: Toward simulation of natural development based on decellularization. *Journal of Tissue Engineering and Regenerative Medicine* **12**, 1432-1447, doi:10.1002/term.2676 (2018).

143 Taylor, D. A., Frazier, O. H., Elgalad, A., Hochman-Mendez, C. & Sampaio, L. C. Building a Total Bioartificial Heart: Harnessing Nature to Overcome the Current Hurdles. *Artificial Organs* **42**, 970-982, doi:10.1111/aor.13336 (2018).

144 Paccola Mesquita, F. C., Hochman-Mendez, C., Morrissey, J., Sampaio, L. C. & Taylor, D. A. Laminin as a Potent Substrate for Large-Scale Expansion of Human Induced Pluripotent Stem Cells in a Closed Cell Expansion System. *Stem Cells Int* **2019**, 9704945-9704945, doi:10.1155/2019/9704945 (2019).

145 Liu, S. *et al.* Strategies to Optimize Adult Stem Cell Therapy for Tissue Regeneration. *International journal of molecular sciences* **17**, 982, doi:10.3390/ijms17060982 (2016).

146 Robertson, C., Tran, D. D. & George, S. C. Concise Review: Maturation Phases of Human Pluripotent Stem Cell‐Derived Cardiomyocytes. *STEM CELLS* **31**, 829-837, doi:10.1002/stem.1331 (2013).

147 Mathur, A. *et al.* Human iPSC-based cardiac microphysiological system for drug screening applications. *Scientific reports* **5**, 8883 (2015).

148 Tulloch, N. L. *et al.* Growth of engineered human myocardium with mechanical loading and vascular coculture. *Circulation research*, CIRCRESAHA. 110.237206 (2011).

149 Nunes, S. S. *et al.* Biowire: a platform for maturation of human pluripotent stem cell-derived cardiomyocytes. *Nat Meth* **10**, 781-787, doi:10.1038/nmeth.2524

http://www.nature.com/nmeth/journal/v10/n8/abs/nmeth.2524.html#supplementary-information (2013).

150 Wang, B. *et al.* Myocardial scaffold-based cardiac tissue engineering: application of coordinated mechanical and electrical stimulations. *Langmuir* **29**, 11109-11117, doi:10.1021/la401702w (2013).

151 Xu, J. *et al.* Micro RNA‐122 suppresses cell proliferation and induces cell apoptosis in hepatocellular carcinoma by directly targeting Wnt/β‐catenin pathway. *Liver international* **32**, 752-760 (2012).

152 Ruffolo Jr, R. R. The pharmacology of dobutamine. *The American journal of the medical sciences* **294**, 244-248 (1987).

153 Motulsky, H. J. & Brown, R. E. Detecting outliers when fitting data with nonlinear regression – a new method based on robust nonlinear regression and the false discovery rate. *BMC Bioinformatics* **7**, 123, doi:10.1186/1471-2105-7-123 (2006).

154 Navarrete, E. G. *et al.* Screening drug-induced arrhythmia using human induced pluripotent stem cell–derived cardiomyocytes and low-impedance microelectrode arrays. *Circulation* **128**, S3-S13 (2013).

155 Feng, Y., Bogaert, J., Oyen, R. & Ni, Y. An overview on development and application of an experimental platform for quantitative cardiac imaging research in rabbit models of myocardial infarction. *Quant Imaging Med Surg* **4**, 358-375, doi:10.3978/j.issn.2223-4292.2013.09.01 (2014).

156 van Spreeuwel, A. *et al.* The influence of matrix (an) isotropy on cardiomyocyte contraction in engineered cardiac microtissues. *Integrative Biology* **6**, 422-429 (2014).

157 Jose, A. D. & Collison, D. The normal range and determinants of the intrinsic heart rate in man. *Cardiovascular research* **4**, 160-167 (1970).

158 Clarke, J., Shelton, J. R., Venning, G. R., Hamer, J. & Taylor, S. THE RHYTHM OF THE NORMAL HUMAN HEART. *The Lancet* **308**, 508-512, doi:https://doi.org/10.1016/S0140-6736(76)90801-1 (1976).

159 Sacha, J. Interaction between Heart Rate and Heart Rate Variability. *Annals of Noninvasive Electrocardiology* **19**, 207-216, doi:10.1111/anec.12148 (2014).

160 Ramaekers, D., Ector, H., Aubert, A., Rubens, A. & Van de Werf, F. Heart rate variability and heart rate in healthy volunteers. Is the female autonomic nervous system cardioprotective? *European heart journal* **19**, 1334-1341 (1998).

161 Smeets, J., A Allessie, M., Lammers, W., Bonke, F. I. M. & Hollen, J. *The wavelength of the cardiac impulse and reentrant arrhythmias in isolated rabbit atrium. The role of heart rate, autonomic transmitters, temperature, and potassium*. Vol. 58 (1986).

162 Chen, W. C. W. *et al.* Decellularized zebrafish cardiac extracellular matrix induces mammalian heart regeneration. *Science advances* **2**, e1600844-e1600844, doi:10.1126/sciadv.1600844 (2016).

163 Herron, T. J. *et al.* Extracellular Matrix–Mediated Maturation of Human Pluripotent Stem Cell–Derived Cardiac Monolayer Structure and Electrophysiological Function. *Circulation: Arrhythmia and Electrophysiology* **9**, e003638, doi:doi:10.1161/CIRCEP.113.003638 (2016).

164 Ross, R. S. & Borg, T. K. Integrins and the myocardium. *Circulation research* **88**, 1112-1119 (2001).

165 Caluori, G. *et al.* Non-invasive electromechanical cell-based biosensors for improved investigation of 3D cardiac models. *Biosensors and Bioelectronics* **124**, 129-135 (2019).

166 Friedrich, O. *et al.* Stretch in Focus: 2D Inplane Cell Stretch Systems for Studies of Cardiac Mechano-Signaling. *Frontiers in Bioengineering and Biotechnology* **7** (2019).

167 Morgan, K. Y. & Black III, L. D. Mimicking isovolumic contraction with combined electromechanical stimulation improves the development of engineered cardiac constructs. *Tissue Engineering Part A* **20**, 1654-1667 (2014).

168 Tan, S. H. & Ye, L. Maturation of pluripotent stem cell-derived cardiomyocytes: a critical step for drug development and cell therapy. *Journal of cardiovascular translational research* **11**, 375-392 (2018).

169 Barbuti, A., Benzoni, P., Campostrini, G. & Dell'Era, P. Human derived cardiomyocytes: A decade of knowledge after the discovery of induced pluripotent stem cells. *Developmental Dynamics* **245**, 1145-1158, doi:10.1002/dvdy.24455 (2016).

170 Ribeiro, M. C. *et al.* Functional maturation of human pluripotent stem cell derived cardiomyocytes in vitro – Correlation between contraction force

and electrophysiology. *Biomaterials* **51**, 138-150, doi:https://doi.org/10.1016/j.biomaterials.2015.01.067 (2015).

171 Organization, W. H. Global action plan for the prevention and control of noncommunicable diseases 2013-2020. (2013).

172 Heron, M. P. Deaths: Leading causes for 2016. (2018).

173 Gongora, C. A. *et al.* Racial and Ethnic Disparities of Heart Transplant Patients and Donors in United States a 2007 to 2016 UNOS Database Analysis. *Circulation* **138**, A15718-A15718 (2018).

174 Zafar, F. *et al.* Pediatric heart transplant waiting list mortality in the era of ventricular assist devices. *The Journal of Heart and Lung Transplantation* **34**, 82-88 (2015).

175 Duisit, J. *et al.* Decellularization of the porcine ear generates a biocompatible, nonimmunogenic extracellular matrix platform for face subunit bioengineering. *Annals of surgery* **267**, 1191-1201 (2018).

176 Becker, M. *et al.* Towards a novel patch material for cardiac applications: tissue-specific extracellular matrix introduces essential key features to decellularized amniotic membrane. *International journal of molecular sciences* **19**, 1032 (2018).

177 Taylor, D. A., Elgalad, A. & Sampaio, L. C. What will it take before a bioengineered heart will be implanted in patients? *Current opinion in organ transplantation* **23**, 664-672 (2018).

178 Oikonomopoulos, A., Kitani, T. & Wu, J. C. Pluripotent stem cell-derived cardiomyocytes as a platform for cell therapy applications: progress and hurdles for clinical translation. *Molecular Therapy* **26**, 1624-1634 (2018).

179 Veerman, C. C. *et al.* Immaturity of human stem-cell-derived cardiomyocytes in culture: fatal flaw or soluble problem? *Stem cells and development* **24**, 1035-1052 (2015).

180 Taylor, D. A. From stem cells and cadaveric matrix to engineered organs. *Current opinion in biotechnology* **20**, 598-605 (2009).

181 Golpanian, S., Wolf, A., Hatzistergos, K. E. & Hare, J. M. Rebuilding the damaged heart: mesenchymal stem cells, cell-based therapy, and engineered heart tissue. *Physiological reviews* **96**, 1127-1168 (2016).

182 Janson, I. A. & Putnam, A. J. Extracellular matrix elasticity and topography: Material‐based cues that affect cell function via conserved mechanisms. *Journal of Biomedical Materials Research Part A* **103**, 1246-1258 (2015).

183 Paez‐Mayorga, J. *et al.* Bioreactors for cardiac tissue engineering. *Advanced healthcare materials*, 1701504 (2018).

184 McGregor, C. G. & Byrne, G. W. Porcine to human heart transplantation: is clinical application now appropriate? *Journal of immunology research* **2017** (2017).

185 Mohiuddin, M. M., Reichart, B., Byrne, G. W. & McGregor, C. G. Current status of pig heart xenotransplantation. *International Journal of Surgery* **23**, 234-239 (2015).

186 Tzatzalos, E., Abilez, O. J., Shukla, P. & Wu, J. C. Engineered heart tissues and induced pluripotent stem cells: macro-and microstructures for disease modeling, drug screening, and translational studies. *Advanced drug delivery reviews* **96**, 234-244 (2016).

187 Shaheen, N., Shiti, A. & Gepstein, L. Pluripotent stem cell‐based platforms in cardiac disease modeling and drug testing. *Clinical Pharmacology & Therapeutics* **102**, 203-208 (2017).